Doctoral Dissertation

Improvement of the operational simplicity of *in vitro* bioconversion systems with thermophilic enzymes

Pham Huynh Ninh

December 2014

Department of Biotechnology

Graduate School of Engineering, Osaka University

TABLE OF CONTENTS

1. General introduction **1**

1.1 Industrial application of enzymes 1

1.1.1 Food processing 1

1.1.2 Pharmaceuticals and cosmetic production 8

1.1.3 Industrial production of biocommodities and biodiesel 13

1.2 *In vitro* metabolic engineering 17

1.3 *In vitro* metabolic engineering with thermophilic enzymes 25

1.4 Objective of this study 30

1.4.1 Thermolysis of *E. coli* cells harboring thermophilic enzymes 30

1.4.2 Co-expression of multiple thermophilic enzymes in a single *E. coli* cell 32

2. Development of a continuous bioconversion system using a thermophilic whole-cell biocatalyst **33**

2.1 Introduction 33

2.2 Materials and Methods 36

2.2.1 Bacterial strain and culture conditions 36

2.2.2 Glutaraldehyde treatment 37

2.2.3 Enzyme assay 37

2.2.4 Heat-induced leakage of *Tt*FTA 39

2.2.5 Electron microscopic analysis 39

2.2.6 Effect of heat treatment on the membrane permeability of GA-treated *E. coli* cells 40

2.2.7 Reusability of GA-treated cells 41

2.2.8 Malate production in continuous reactor using GA-treated cells 42

2.3 Results 44

2.3.1 Effects of GA treatment on heat induced leakage of *Tt*FTA 44

2.3.2 Electron microscopic analysis 47

2.3.3 Membrane permeability of GA-treated cells 49

2.3.4 Reusability of GA-treated cells in repeated batch reactions 51

2.3.5 Continuous bioconversion using GA-treated cells as whole-cell catalysts 52

2.4 Discussion 54

2.5 Summary 57

3. Assembly and multiple gene expression of thermophilic enzymes in *Escherichia coli* for *in vitro* metabolic engineering 58

3.1 Introduction 58

3.2 Materials and Methods 60

3.2.1 Bacterial strains 60

3.2.2 Plasmid construction 60

3.2.3 Gene assembly 62

3.2.4 Real-time PCR 63

3.2.5 Enzyme assay 66

3.2.6 Determination of pyruvate production rate 67

3.2.7 Lactate production 68

3.2.8 Analytical methods 69

3.3 Results and Discussion 70

3.3.1 Gene assembly 70

3.3.2 Expression profile of the assembled genes 74

3.3.3 Determination of the flux through the *in vitro* metabolic pathway 80

3.3.4 Lactate production through the *in vitro* metabolic pathway 82

3.4 Summary 86

4. Conclusions and future aspects 87

References 92

Supplementary Fig S1 103

Supplementary Fig S2 108

Related Publications 109

Presentations in Conferences 110

Acknowledgements 111

ABBREVIATIONS

(S)-MEOIPA	(*S*)-methoxyisopropylamine
3-PGA	3-phospho-D-glycerate
7-ADCA	7-amino deacetoxy cephalosporanic acid
ADH	Alcohol dehydrogenase
ADP	Adenosine diphosphate
AlDH	Glyceraldehyde dehydrogenase
ALS	Acetolactate synthase
ATP	Adenosine triphosphate
Dex3, Dex40	Dextrans with average molecular weight of 3 or 40 kDal
DFA III	Disacchride difructose anhydride III
DHAD	Gluconate/glycerate/dihydroxyacid dehydratase
EM	Emben-Meyerhof
EMR	Epimerase
ENO	Enolase
FBA	Fructo-biphosphate aldolase
FTA	Fumarase
GA	Glutaraldehyde

GAPDH	Glycerate phosphate dehydrogenase
GAPN	Non-phosphorylating glyceldehyde-3-phosphate dehydrogenase
GDH	Glucose dehydrogenase
GK	Glucose kinase
GOS	Galacto-oligosaccharides
HPLC	High-performance liquid chromatography
IPTG	Isopropyl β-D-1-thiogalactopyranoside
KARI	Ketolacid reductoisomerase
KDC	2-ketoacid decarboxylase
KDGA	2-keto-3-deoxygluconate aldolase
LB	Luria-Bertani
LDH	Lactate dehydrogenase
ME	Malic enzyme
Me	Methinonine
MGE	Multiple-gene-expression
MLDH	Malate/lactate dehydrogenase
NAD^+/NADH	Nicotinamide adenine dinucleotide
$NADP^+$/NADPH	Nicotinamide adenine dinucleotide phosphate

PAA	Phenyl acetic acid
PDC	Pyruvate decarboxylase
PFK	6-phosphofructose kinase
PGA	Penicillin G acylases
PGK	Phosphoglycerate kinase
PGM	Cofactor-independent phosphoglycerate mutase
PGI	Glucose-6-phosphate isomerase
PK	Pyruvate kinase
PRK	Phosphoribulokinase
Phe	Phenylalanine
RBS	Ribosome binding site
RT-PCR	Real time PCR
RuBP	D-ribulose-1,5-bisphosphate
SEM	Scanning electron microscopy
SGE	Single-gene-expression
TEM	Tranmission electron microscopy
TIM	Triose phosphate isomerase
TKL	Transketolase

1. General introduction

1.1 Industrial application of enzymes

Microbial enzymes play a crucial role as catalysts in the food, chemical, and pharmaceutical industries owing to their high reaction selectivity and ability to accept a wide range of complex molecules as substrates. Consequently, they can be used in both simple and complex transformations in numerous commercial applications. The global market for industrial enzymes was worth nearly US $4.8 billion in 2013 and is expected to reach around US $7.1 billion by 2018 (BBC research, 2014). Industrial bioconversions using single enzyme or a few enzymes have been matured as a well-developed technology and commercially employed in the field of food processing, pharmaceutical and cosmetic production, and the industrial production of commodity chemicals. Over 500 industrial products were produced through the enzymatic modifications (Johannes et al., 2006).

1.1.1 Food processing

Food production is the largest segment of industrial application of enzymes. The applications of enzymes can be found in almost every sector of this field such as confectionary and sweeteners, dairy, dietary and beverages. Many enzymes have been

commercially used in this filed such as amylase, protease, lipase, cellulose and catalase. Among these, amylases seem to be the most widely used enzymes in the field of food processing. For example, more than 10 million tons of isomerized sugar syrup has been produced through an enzymatic digestion of starches with amylase followed by the further hydrolysis of sugar oligomers by glucoamylase, and the isomerization of resulting glucose into fructose with glucose isomerase (DiCosimo et al., 2013) (Scheme 1). The bacterial glucose isomerase, fulgal α-amylase, and glucoamylase are currently used to produce "high fructose corn syrup" from starch in a US $1 billion business (Adrio et al., 2014).

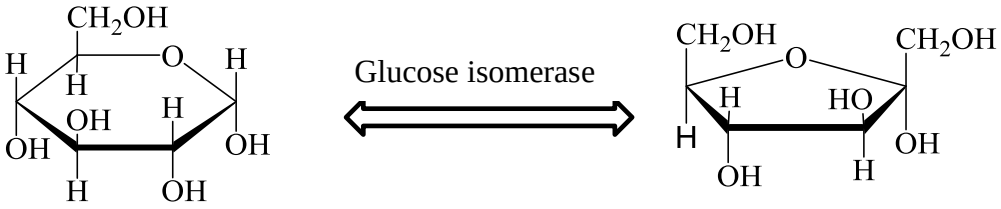

Glucose (aldose)
75 % as sweet as sucrose

Fructose (ketose)
160% as sweet as sucrose

Scheme 1: Isomerization of D-glucose to D-fructose

Another example is the production of L-aspartyl-L-phenylalanine methyl ester or aspartame (Scheme 2), which is an artificial low-calorie sweetener. Aspartame is widely

used as a sugar substitute in some foods and beverages. The global production of this peptide sweetener, with an about 200-times sweeter than sucrose, has been estimated more than 25,000 tons in 2014 (Ajinomoto, 2013). The low-calorie sweetener aspartame is produced on a ton scale by Holland Sweetener Company, a joint venture of Tosoh and DSM. The aspartame process uses thermolysin to catalyze the formation of the dipeptide bond from N-protected L-aspartic acid (Benzyloxycarbonyl-L-aspartate) and DL-phenylalanine methyl ester (Schmid et al., 2001).

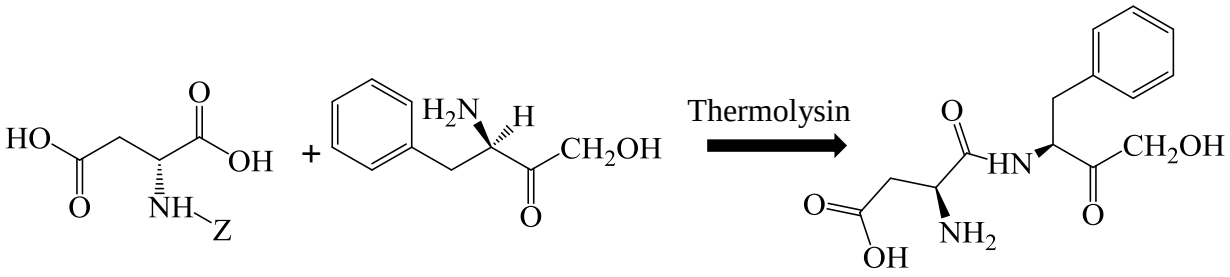

Benzyloxycarbonyl-L-aspartate

L-Phenylalanine-methyl ester

Aspartame

Scheme 2: Aspartame production process (a peptide bonding catalyzed by thermolysin).

In the dairy industry, proteases have long been applied for the manufacture of cheese. They were used to hydrolyze the specific peptide bond (Phe105-Met106) that generates para-kappa-casein and macropeptides (Rao et al., 1998). The proteases were also used to produce the low allergenic milk protein used as ingredients in baby milk

formulas (Gupta et al., 2002). Another application of enzymes in dairy industry is the production of lactose-free milk or skim milk. The immobilized β-galactosidase was used for the hydrolysis of lactose in production of skim milk (Scheme 3). The first company conducted the commercial hydrolysis of lactose in milk by using immobilized lactase was Centrale del Latte of Milan, Italy (Panesar et al., 2010). The process used an immobilized *Saccharomyces* (*Kluyveromyces*) *lactis* lactase entrapped in cellulose triacetate fibers.

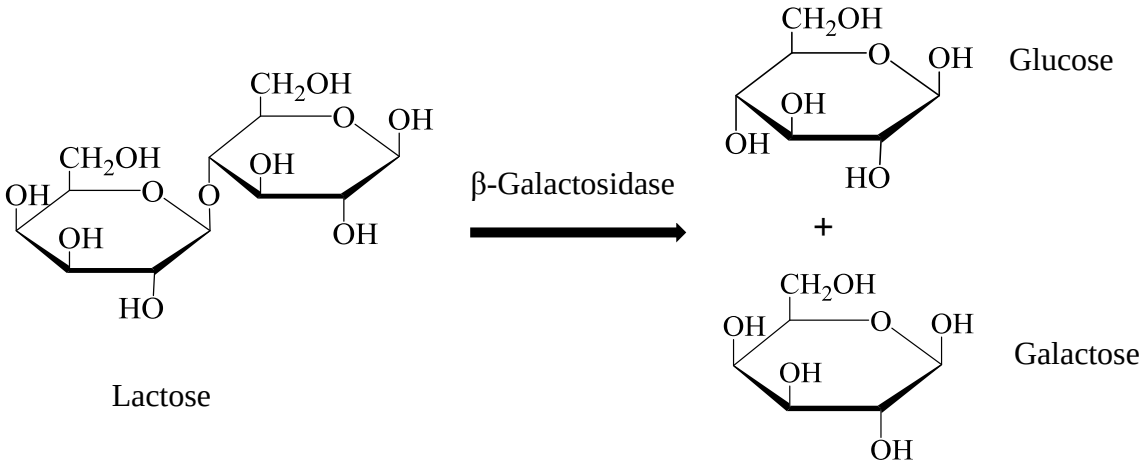

Scheme 3: Lactose hydrolysis by β-galactosidase

The enzyme β-galactosidase was also applied for the industrial production of oligosaccharides. Oligosaccharides are non-digestible saccharides polymers containing 3-10 monomeric sugar units, which were used as prebiotics in human food. For example, galacto-oligosaccharides (GOS), a member of oligosaccharides, are usually produced

from lactose via enzymatic synthesis with β-galactosidases (Playne et al., 2009) (Scheme 4). GOS are currently used in a wide range of food and beverage products, such as infant formulas, dairy products, sauces, soups, breakfast cereals, beverages, snack bars, ice creams, bakery products, animal feeds, and sugar replacements. The production of lactose-derived oligosaccharides (GOS, lactulose, and lactosucrose) is estimated to be 20,000 - 32,000 tons (Gänzle, 2012).

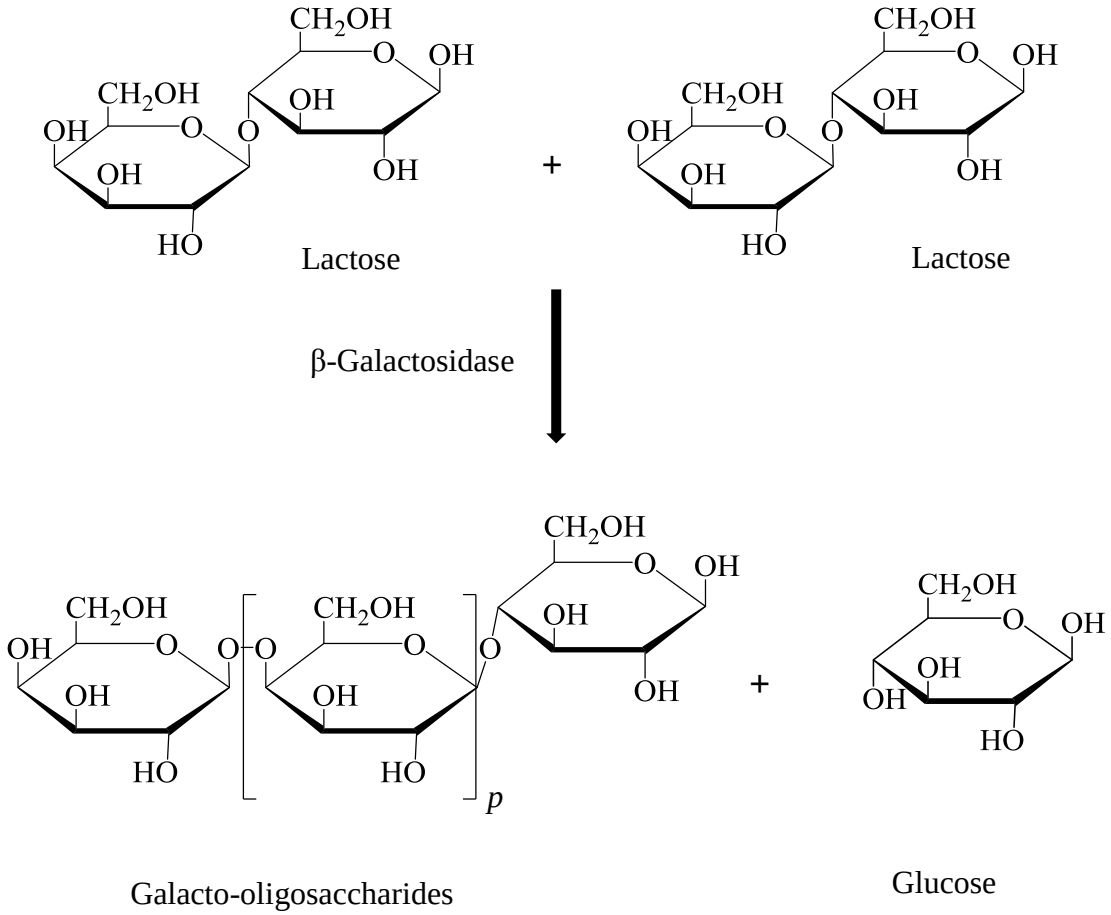

Scheme 4: Galacto-oligosaccharides production using β-galactosidase (p = 1-6).

Disaccharide difructose anhydride III (DFA III), a non-reducing, non-cariogenic sweetener with prebiotic properties, is also one of the food chemicals being synthesized by enzymes modification (Scheme 5). Recent research on DFA III showed its ability to reduce the formation of secondary bile acids in the human large intestine (Minamida et al., 2006), which is considered to be beneficial in preventing colon cancer. In addition, DFA III was found to enhance calcium absorption in humans (Shigematsu et al., 2004). DFA III has been industrially manufactured using commercially available purified inulin and *Arthrobacter* sp. H65-7 fructosyltransferase (Inulase II) at the Shimizu Factory of Nippon Beet Sugar, Tokyo, Japan, since 2004 (Kikuchi et al., 2009).

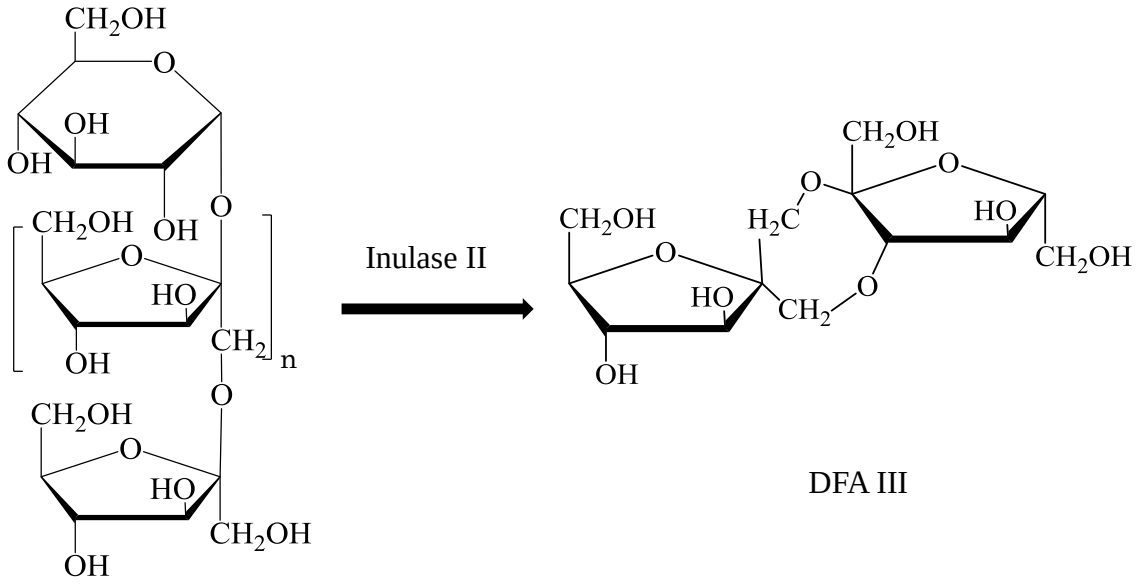

Scheme 5. Enzymatic production of difructose dianhydride III (DFA III) from Inulin.

Another industrial application of enzymes in food processing is the production of structured lipids. Structured lipids are tailor-made fats and oils which incorporate specific new fatty acids to triacylglycerols, or have different compositions and positional distribution of existing fatty acids, within its glycerol backbone. The lipase-mediated interesterification of food oils and fats allows the control of final product compositions. The interesterification using lipases has come into practical use to produce oils and fats with desired physical properties and to reduce the content of *trans*-fatty acids. For instance, Alimetos Polar Comercial C.A., in Venezuela reported the start-up an interesterification plant with a capacity of 80 tons per day in 2009 (Dicosimo et al., 2013). The interesterification approach using lipases was used to produce a commercial vegetable fat blend, namely Betapol® (Loders Croklaan, Glen Ellyn, Ill., U.S.A.), which has been developed for infant formulas (Osborn et al., 2002).

Enzymes (e.g. amylases, hemicellulases, amyloglucosidase, proteases) are also used in baking industry to provide specific properties in the flour and dough or to lower the protein level of flour for biscuits and crackers. Amylases and hemicellulases are applied to improve and standardize the quality of the bread (e.g. softness, volume, crumb quality). Others enzymes useful in the food processing include invertase for candy and jam production (Adrio et al., 2014). Recently, intensive works have been carried out on

the application of transglutaminase as a texturing agent in the processing of, for example, sausages, noodles and yoghurt, where cross-linking of proteins provides improved viscoelastic properties of the products (Kieliszek et al., 2014).

1.1.2 Pharmaceuticals and cosmetic production

β-Lactam antibiotics are one of the most widely used pharmaceuticals and some of them are produced by the enzymatic modification with penicillin G acylases (PGA). PGA acts on the side chain of penicillin G and cephalosporin G to produce antibiotic intermediates, including 6-amino penicillanic acid (6-APA), 7-amino deacetoxy cephalosporanic acid (7-ADCA) with a release of phenyl acetic acid (PAA) as a by-product (Scheme 6). These antibiotic intermediates are the building blocks of semi-synthetic penicillins (ampicillin, amoxicillin, cloxacillin) and cephalosporins (Arroyo et al., 2003; Elander, 2003). Among them, the annual production yield of 7-ADCA is estimated to be 300 tons (Muñoz Solano et al., 2012).

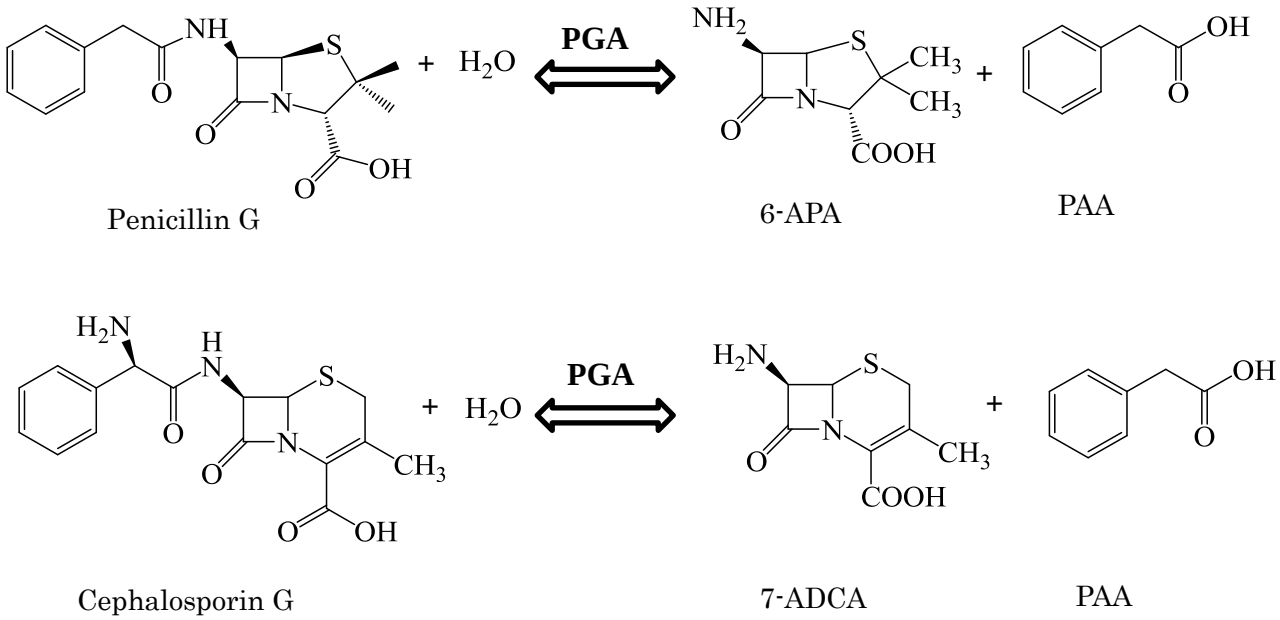

Scheme 6: Enzymatic conversion of penicillin G and cephalosporin G to 6-APA and 7-ADCA.

The excellent regio-, and enantio-specificity of enzymes enables the selective production of chemically indistinguishable isomers and is often used for the production of chiral compounds which can serve as building blocks for pharmaceutical synthesis. Enantiomerically pure amino acids, amino alcohols, amines, and alcohols play an increasingly important role as intermediates in the pharmaceutical industry, where both a high level of purity and abundant quantities of the compounds are required. Esterases, lipases, proteases, and ketoreductases are wildly applied for the preparation of chiral alcohol, amines, carboxylic acid, and others. Several methods have been developed for

the enantioselective synthesis of chiral alcohols, such as enzyme-catalyzed kinetic resolution of racemic substrates, asymmetric reduction of prochiral ketones, and asymmetric hydroxylation of hydrocarbons. One of the most successful examples in this field is the production of atorvastatin by the asymmetric reduction of prochiral alcohol. Atorvastatin, the active ingredient in Lipitor, is a cholesterol-lowering drug that had global sale of US $11.9 billion in 2010 (Bornscheuer et al., 2012). Ethyl (*R*)-4-cyano-3-hydroxybutyric acid, a key intermediate for the synthesis of atorvastatin, was prepared through an enzymatic process which based on ketoreductase, glucose dehydrogenase and halohydrin dehalogenase (Patel, 2013) (Scheme 7).

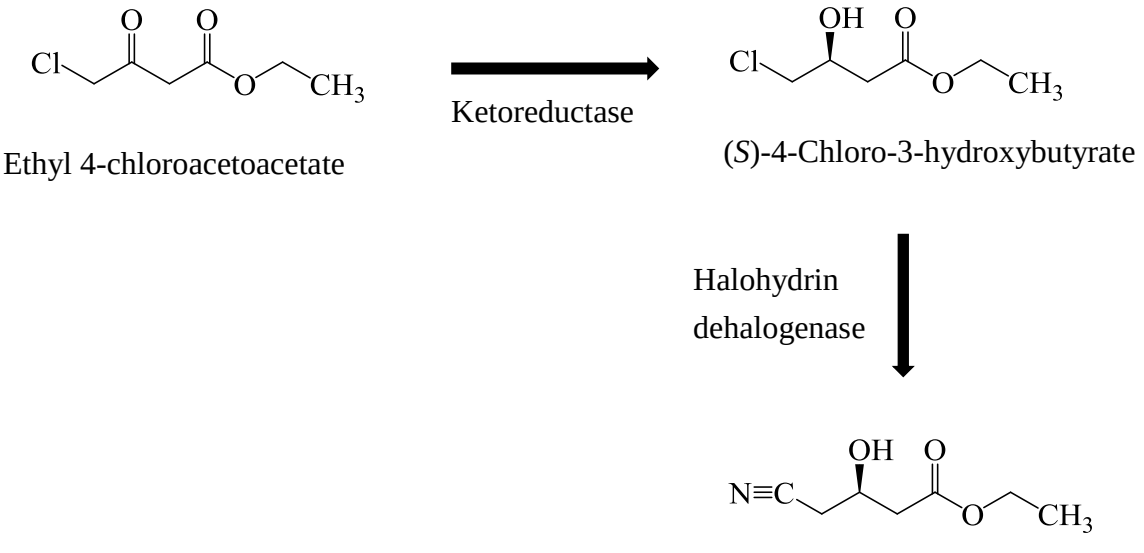

Ethyl 4-chloroacetoacetate

(*S*)-4-Chloro-3-hydroxybutyrate

Ethyl (*R*)-4-cyano-3-hydroxybutyrate

Scheme 7: Enzymatic preparation of (*R*)-4-Cyano-3-hydroxybutyrate

Kinetic resolution of racemic amines is a common method used in the synthesis of chiral amines. Lipase-catalyzed acylation of a primary amine moiety can be used for the optical resolution of racemic primary amines. BASF company successfully developed the process, which is operated on a multi-thousand ton scale, for the synthesis of a variety of enantiopure amines. One example of the optically active amine bioconversion is the production of (*S*)-methoxyisopropylamine ((*S*)-MEOIPA) (Scheme 8). It is a building block for a herbicide, Frontier x2, and was produced with an annual yield of 2,000 tons (Schmid et al., 2001). The intermediate (*S*)-methoxyisopropylamine is synthesized via transamination of methoxyacetone with isopropylamine.

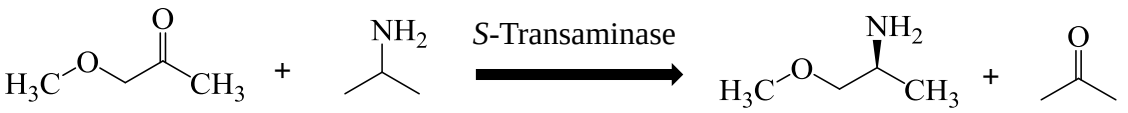

Methoxyacetone Isopropylamine (*S*)-MEOIPA Acetone

Scheme 8: Synthesis of (*S*)-methoxyisopropylamine

Preparation of chiral carboxylic acids is another industrial application of enzymes. (*R*)-*o*-Chloromandelic acid is an important chiral intermediate for the production of a platelet aggregation inhibitor named Clopidogrel®, a drug to prevent heart attacks and

strokes with a global sale of US $10 billion per year (Zheng et al., 2011). Enzymatic synthesis of (*R*)-*o*-chloromandelonitrile is the key step in the synthesis of (*R*)-*o*-chloromandelic acid. This reaction was carried out in microaqueous or biphasic systems and the produced (*R*)-*o*-chloromandelonitrile can then be converted into (*R*)-*o*-chloromandelic acid without racemization (Scheme 9).

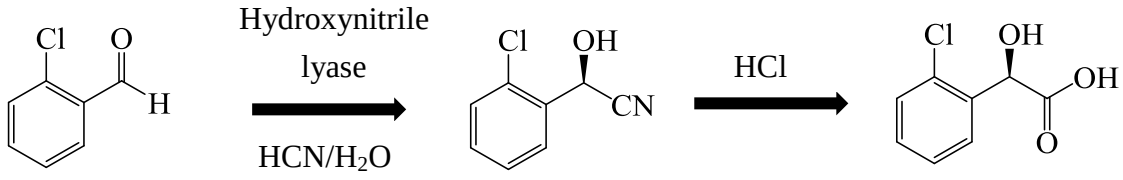

o-Chlorobenzaldehyde (*R*)-*o*-Chloromandelonitrile (*R*)-*o*-Chloromandelic acid

Scheme 9: Synthesis of (*R*)-*o*-chloromandelic acid via hydroxynitrile lyase

In cosmetic industry, great expectations are attributed to the application of enzymes in skin care. Enzymes with the ability to capture free radicals were used to prevent the damages by environment, bacteria, sunlight or other harmful factors to the skin. A combination of superoxide dismutase and peroxidase was used as in cosmetic products to reduce UV-induced erythema (Lods et al., 2000).

1.1.3 Industrial production of biocommodities and biodiesel

Enzymes are also applied to the chemical industry as catalysts. Although applications of enzymes in chemical industries are mainly focused on the production of fine chemicals, there are a few examples where the enzymes are also used to produce commodity chemicals. The enzymatic hydration of acrylonitrile to acrylamide using an immobilized bacterial enzyme, nitrile hydratase is the most successful example in this field and its annual yield is more than 100,000 tons worldwide (Vandamme et al., 2004). The enzymatic conversion of acrylonitrile to acrylamide is illustrated in Scheme 10. In this reaction, a nitrile hydratase catalyzes the transformation of a cyanide group into an amide. Acrylamide is then polymerized to polyacrylamide. This process was one of the first large-scale applications of enzymes in the bulk chemical industry and replaces the conventional chemical production process that uses sulfuric acid and inorganic catalysts.

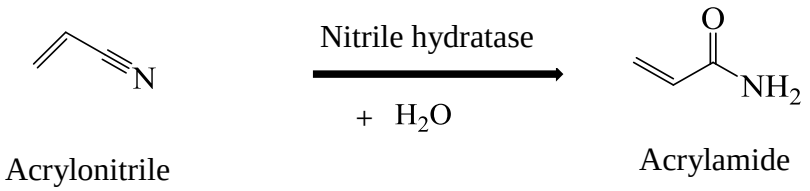

Acrylonitrile Acrylamide

Scheme 10: Enzymatic conversion of acrylonitrile to acrylamide by a nitrile hydratase

Another example is the production of L-amino acids. Industrial exploitation of enzymes has also long been applied for production of L-amino acids and their derivatives. For instance, Degussa produces L-*tert*-leucine from ammonium formate and trimethylpyruvic acid at a ton scale using an enzyme couple of L-leucine dehydrogenase and formate dehydrogenase (Bommarius et al., 1995) (Scheme 11). The cofactor (NADH) must be regenerated in a further redox reaction because of their high cost. In this process, a formate dehydrogenase from *Candia boidinii*, which oxidizes formate irreversibly to CO_2 using NAD^+, was used to regenerate NADH from NAD^+.

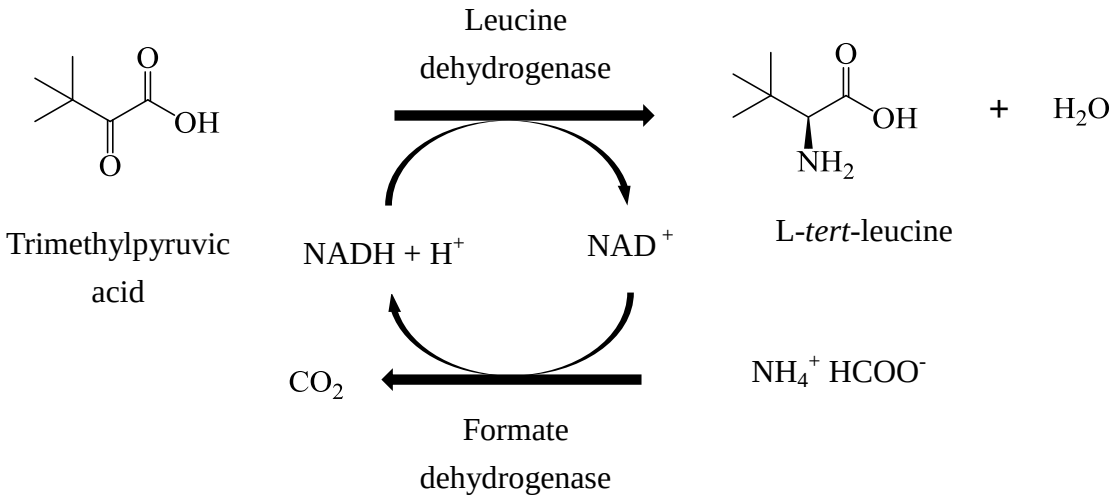

Scheme 11: Production of L-*tert*-leucine through reductive amination with leucine dehydrogenase.

A variety of proteinogenic (alanine, methionine, valine, tryptophan) and non-proteinogenic amino acids (*o*-benzylserine, norleucine, norvaline) have been prepared at Degussa in bulk quantities by the resolution of the corresponding *N*-acetyl amino acids. For example, L-methionine, which is required for the production of infusion solutions and special diets, was produced by the enzymatic resolution with an acylase in an enzyme membrane reactor to minimize enzyme consumption (Scheme 12). After the acylase resolution, the L-methionine is isolated from the reaction mixture by an ion chromatography and purified by crystallization. Several hundred tons of L-methionine are now produced each year using the enzyme membrane reactor technology (Woeltinger et al., 2005).

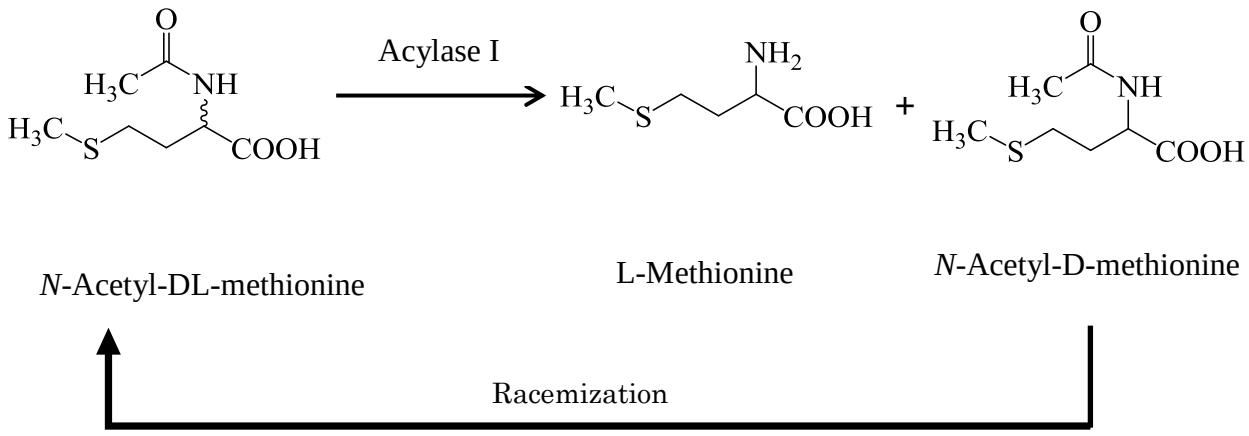

Scheme 12: L-Methionine production via the acylase route.

Another commodity chemical produced by an enzymatic conversion is biodiesel. Biodiesel has attracted much more attention in recent years because of its biodegradability, environmentally friendliness, and renewability. The biochemical catalysis method has been developed in the past decade and many immobilized enzymes are commercially available to meet the large-scale industrialization of biodiesel production. The most method used to produce enzymatic biodiesel is the transesterification of oil by lipase with an alcohol as acyl acceptor (Scheme 13). The lipase-catalyzed synthesis of biodiesel offers some advantages, such as working under gentle conditions and with various triglyceride substrates (e.g., waste oil and fats), easy recovering of biocatalyst and glycerol, and low environmental impacts (de Regil et al., 2013). In 2006, Hainabaichuan Co. Ltd., Hunan Province, China conducted an enzymatic production process for biodiesel with a capacity of 20,000 tons/per year (enlarged to 40,000 tons/per year in 2008) using Novozyme 435 (immobilized lipase) as the catalyst. Waste palm oil, waste edible oil, and oil with high acid value could be used as starting materials of this process (Zhang et al., 2012).

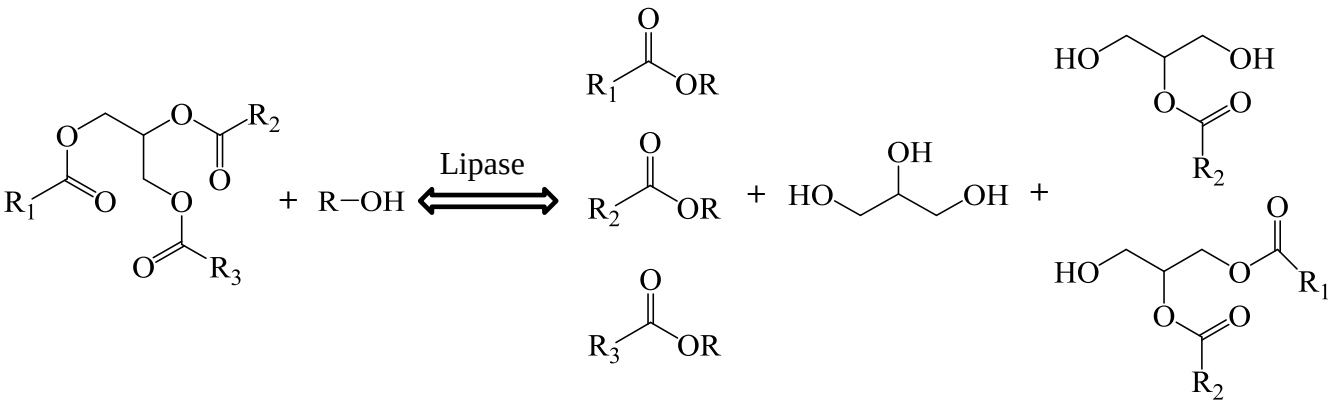

Scheme 13: Enzymatic transesterification of oils with alcohol to produce biodiesel.

1.2 *In vitro* metabolic engineering

As mentioned in the previous section, a number of industrial processes, in which a single or few enzymes are used as catalyst(s), have been developed so far. On the other hand, a relatively novel approach, in which a certain number (more than 3) of enzymes are combinatorially used in a single batch, has been recently developed and applied to the production of industrial chemicals at a lab scale. This approach, designated as *in vitro* metabolic engineering in this thesis, offers some distinct advantages over conventional fermentation-based processes. For instance, it shows great engineering flexibility without considering cellular viability and membrane, high product yields without by-products, fast reaction rates, broad reaction conditions (e.g., presence of

organic solvents or microbe-toxic compounds), and industrial scalability (Zhang et al., 2011). Moreover, implementation of cascade reaction in a simple buffer solution leads to the elimination of the use of culture media and easy downstream processes.

In vitro metabolic engineering approach has been applied for the lab-scale production of various chemical products, including biofuels, biocommodities, and even bio-electricity. For examples, Bae and coworkers (1999) reported the production of aromatic D-tyrosine in the enzymatic conversion system comprising four enzymes, namely, glutamate racemase, D-amino acid transferase, glutamate dehydrogenase, and formate dehydrogenase (Scheme 14). D-Tyrosine was produced from the corresponding D-keto acid (hydroxyphenylpyruvate) and D-glutamate by D-amino acid aminotransferase. D-Glutamate is continuously regenerated by the coupled reactions of glutamate dehydrogenase and glutamate racemase from α-ketoglutarate, NADH and ammonia. NADH is regenerated by formate dehydrogenase. This system showed an effective approach for D-amino acid production without undesired side products.

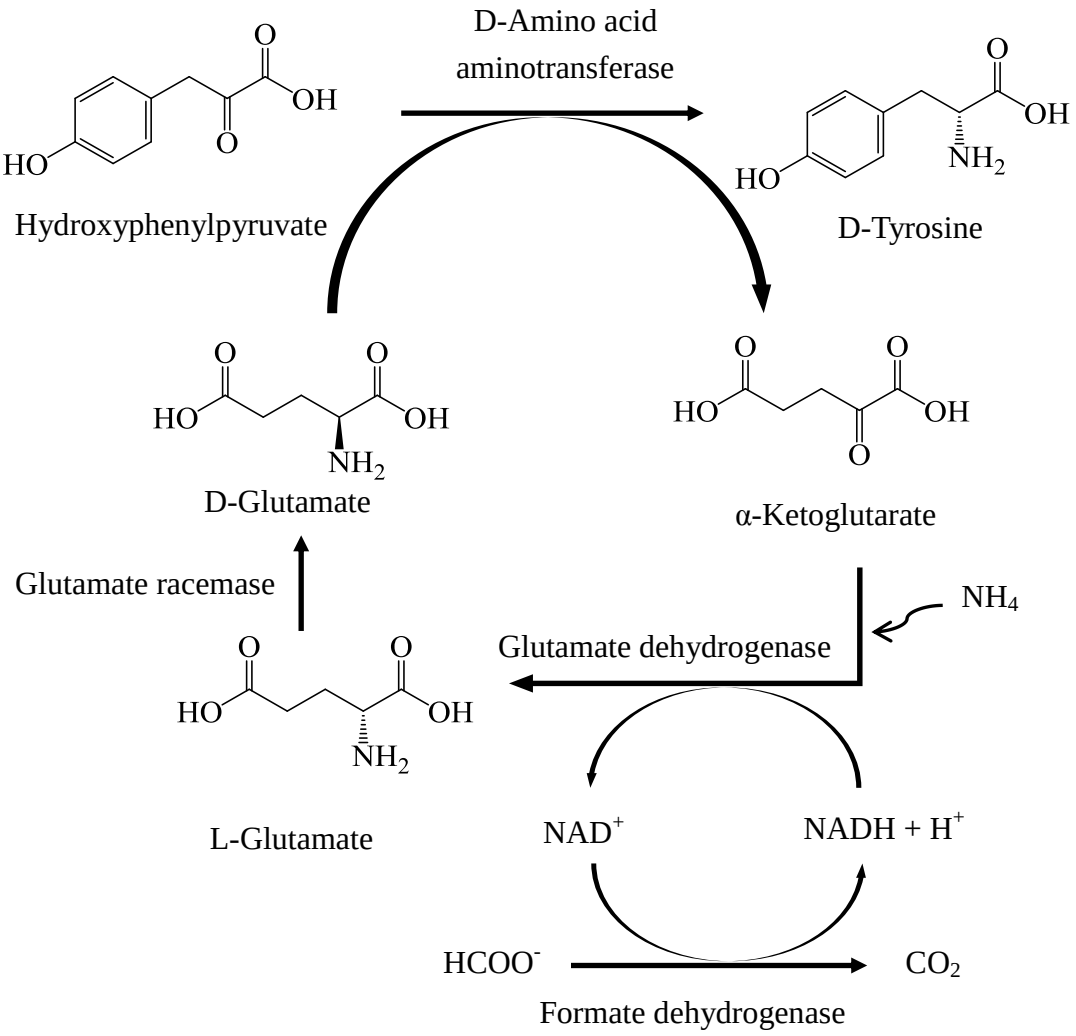

Scheme 14: Biosynthesis of D-tyrosine with four-enzyme system.

The production of riboflavin isotopomers from ribulose 5-phosphate through a synthetic enzymatic pathway involving 8 isolated enzymes is another application of *in vitro* metabolic engineering approach (Römisch et al., 2002). Six enzymes are involved in the synthesis of riboflavin isotopomers (i.e., hexokinase, glucose-6-phosphate

dehydrogenase, 6-phospho-gluconate dehydrogenase, 3,4-dihydroxy-2-butanone 4-phosphate synthase, 6,7-dimethyl-8-ribityllumazine synthase, and riboflavin synthase) and two auxiliary enzymes (pyruvate kinase and glutamate dehydrogenase) mediate regeneration of ATP and $NADP^+$. The overall yields of riboflavin isotopomers were 35-50 mol% for 3-days incubation at 37^oC. The relatively long incubation time, which may cause the loss of phosphate residues from intermediates by residual phosphatase activities present in the commercial enzymes, was assumed as the reason for the low production yield of riboflavin isotopomers.

The *in vitro* metabolic engineering approach was also applied for the production of D-3-phosphoglycerate through a series of eleven packed-bed reactors containing immobilized enzymes (Bhattacharya et al., 2004). A novel scheme employing enzymatic catalysts including phosphoglycerate kinase (PGK), glycerate phosphate dehydrogenase (GAPDH), triose phosphate isomerase (TIM), aldolase, transketolase (TKL), phosphatase (FBPase/SBPase), epimerase (EMR), and phosphoribulokinase (PRK) was developed for the conversion of D-ribulose-1,5-bisphosphate (RuBP) from 3-phospho-D-glycerate (3-PGA) (Scheme 15). The overall conversion yield through the pathway was 56 mol%. It was significantly lower than the 90 mol% predicted from enzyme performance in individual reaction steps. The possible reason is the modulation

of the kinetic properties of the enzymes by residual intermediates, cofactors, and by-products from incomplete enzymatic conversion in upstream steps. Recently, Opgenorth and coworkers (2014) have developed *in vitro* chemical pathways with a simple purge valve module for maintaining $NADP^+$/NADPH balance and used them for the production of polyhydroxybutyryl bioplastic and isoprene from pyruvate with nearly 100 mol% of the theoretical yield.

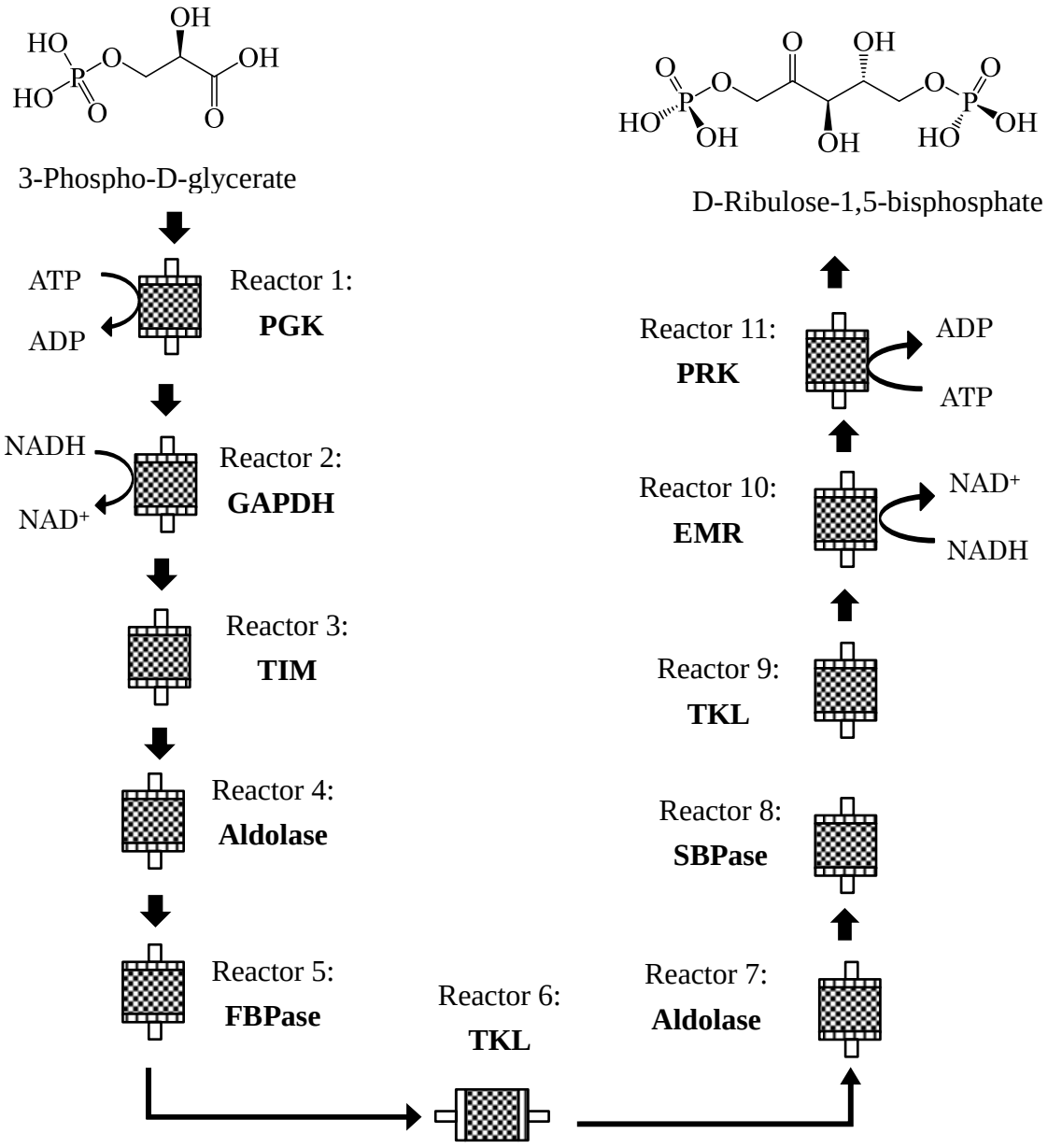

Scheme 15: The schematic diagram of the cascade of eleven immobilized enzyme reactors used for the production of RuBP from 3-PGA.

For biofuel production, Welch and Scopes (1985) reconstituted the glycolytic pathway *in vitro* using 13 purified yeast enzymes and applied it to the ethanol production from glucose. Through this *in vitro* pathway, they could convert 1 M of glucose to ethanol with nearly 100% (mol/mol) yield in 8 h. Guterl et al. (2012) have constructed an artificial glycolytic pathway comprised of only 4 enzymes, namely, glucose dehydrogenase (GDH), gluconate/glycerate/dihydroxyacid dehydratase (DHAD), 2-keto-3-deoxygluconate aldolase (KDGA), and glyceraldehyde dehydrogenase (AlDH) (Scheme 16). By coupling this artificial pathway with pyruvate decarboxylase (PDC) and alcohol dehydrogenase (ADH), they could produce ethanol with a yield of 57.4 mol%. This pathway was also applied to iso-butanol production from glucose by coupling with five other enzymes, namely, acetolactate synthase (ALS), ketolacid reductoisomerase (KARI), dihydroxy acid dehydratase (DHAD), 2-ketoacid decarboxylase (KDC), and alcohol dehydrogenase (ADH) (Scheme 16).

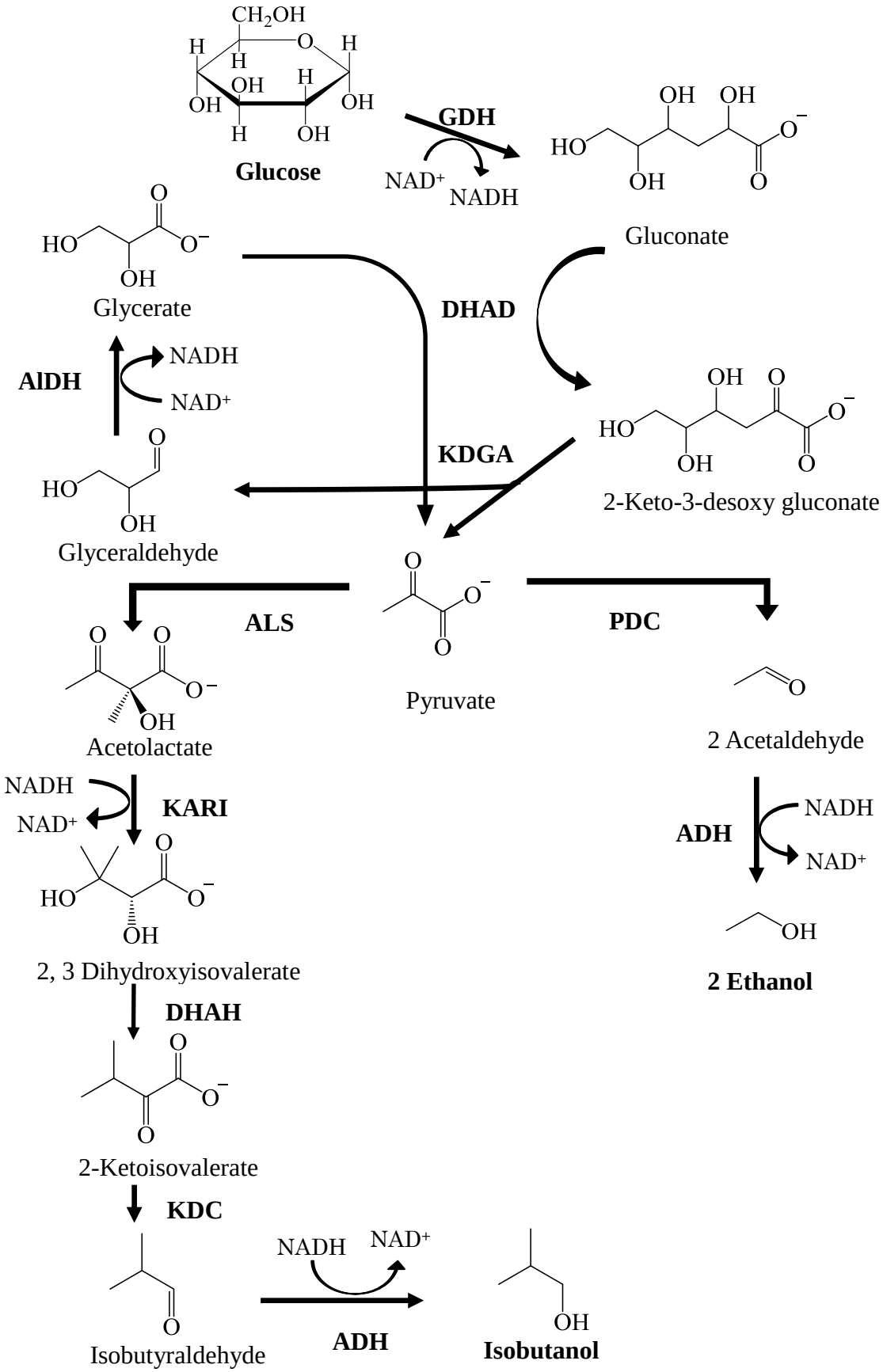

Scheme 16: Enzymatic pathway for the production of ethanol and isobutanol.

The *in vitro* metabolic engineering approach was also applied for the bioelectricity production. Zhu et al. (2014) could produce nearly 24 electrons per glucose unit of maltodextrin in an air-breathing enzymatic fuel cell through a synthetic catabolic pathway comprised of 13 enzymes. The enzymatic fuel cells containing a 15% (w/v) maltodextrin solution have an energy-storage density of 596 Ah kg^{-1}, which is one order of magnitude higher than that of lithium-ion batteries. More recently, Myung et al. (2014) have designed an *in vitro* enzymatic pathway containing 15 enzymes for the hydrogen generation from water and sucrose under mild reaction conditions. The molar yield of hydrogen reached to 96.7% of the theoretical yield (i.e., 12 dihydrogen per hexose) in batch reaction. This study showed that a high-hydrogen generation via enzyme-catalyzed water splitting using sugars as a source of splitting power could be a promising approach for the hydrogen production.

1.3 *In vitro* metabolic engineering with thermotolerant enzymes

In spite of these successful examples, *in vitro* metabolic engineering has not yet come into a practical use. Rollin and coworkers (2013) pointed out that there remain four major challenges toward the industrial application of *in vitro* metabolic engineering, namely (i) low-cost enzyme production, (ii) prolonged enzyme stability, (iii) cofactor

engineering, and (iv) pathway optimization and modeling. The employment of thermotolerant enzymes, which are derived from thermophilic and hyperthermophilic microorganisms, can provide the possible solutions for some of these limitations. The excellent stability of thermophilic enzymes can be exploited to prolong the bioconversion process. In addition, themophilic enzymes expressed in the engineered hosts such as *E. coli* can be simply purified by heat precipitation. Therefore, the low-cost enzymes production can also be achieved. High operational temperature of thermophilic enzymes provides many important advantages to *in vitro* bioconversions, such as better substrate solubility, high mass transfer rate, and low risk of contamination (Turner et al., 2007). A simple heat-treatment of recombinant mesophilic cells (e.g., *Escherichia coli*) harboring thermophilic enzymes results in the denaturation of indigenous proteins and enables one-step preparation of highly selective thermotolerant biocatalytic modules without costly and time-consuming procedure for enzymes purification. In addition, the cell membrane barrier of the mesophilic host is partially or entirely disrupted at high temperature and a better accessibility between enzymes and substrates can be achieved (Giuliano et al., 2004; Ren et al., 2007). More importantly, the excellent stability of thermophilic enzymes can be exploited to overcome the most serious limitation of *in vitro* bioconversions, namely their inability in protein synthesis

and renewal. In principle, this approach is applicable to all thermophilic enzymes as long as they can be functionally produced in an appropriate mesophilic host cells. Therefore, an artificial *in vitro* metabolic pathway for the production of a special chemical can be constructed by a rational combination of enzymes. Using this approach, Honda et al. (2010) constructed an artificial metabolic pathway including 6 thermophilic enzymes for the production of 2-deoxyribose 5-phosphate from fructose. In this research, six recombinant *Escherichia coli* strains producing each of the thermophilic enzymes, namely fructokinase, 6-phosphofructokinase, polyphosphate kinase from *Thermus thermophilus* HB8 and FBP aldolase, triosephosphate isomerase, glycerol 3-phosphate dehydrogenase from *Thermus thermophilus* HB27, were pre-heated at 70^{o}C for 30 min to inactivate the indigenous proteins and then directly used for the production of 2-deoxyribose 5-phosphate from fructose with a molar yield of 55%.

Similarly, Ye et al. (2012, 2013) designed a non-ATP-forming chimeric Emben-Meyerhof (EM) pathway for the production of lactate and malate from glucose (Scheme 17). The chimeric EM pathway with balanced consumption and regeneration of ATP/ADP was constructed by using nine (hyper)thermophilic glycolytic enzymes, namely, glucose kinase (GK), glucose-6-phosphate isomerase (PGI), 6-phosphofructose kinase (PFK), fructo-biphosphate aldolase (FBA), triosephosphate isomerase (TIM),

enolase (ENO), pyruvate kinase (PK) of *Thermus thermophilus*, the cofactor-independent phosphoglycerate mutase of *Pyrococcus horikoshii* (PGM), and the non-phosphorylating glyceldehyde-3-phosphate dehydrogenase (GAPN) of *Thermococcus kodakarensis*. By coupling this pathway with thermophilic malate/lactate dehydrogenase of *Thermus thermophilus* (MLDH) or a thermophilic malic enzyme derived from *Thermococcus kodakarensis* (ME), the direct conversion of glucose to lactate or malate could be achieved, respectively.

More recently, a non-natural, cofactor balanced and oxygen insensitive *in vitro* metabolic pathway was constructed using 16 thermophilic enzymes and used for *n*-butanol production from glucose (Krutsakorn et al., 2013). In this research, 16 recombinant *E. coli* cells having each thermophilic enzyme constituting the *in vitro* metabolic pathway were rationally combined in a single batch for the *n*-butanol production. The metabolic flux through this pathway could be spectrophotometrically monitored. Therefore, the level of each enzyme can be experimentally adjusted to achieve the desired reaction rate. The overall product yield through this optimized pathway was 82 mol%.

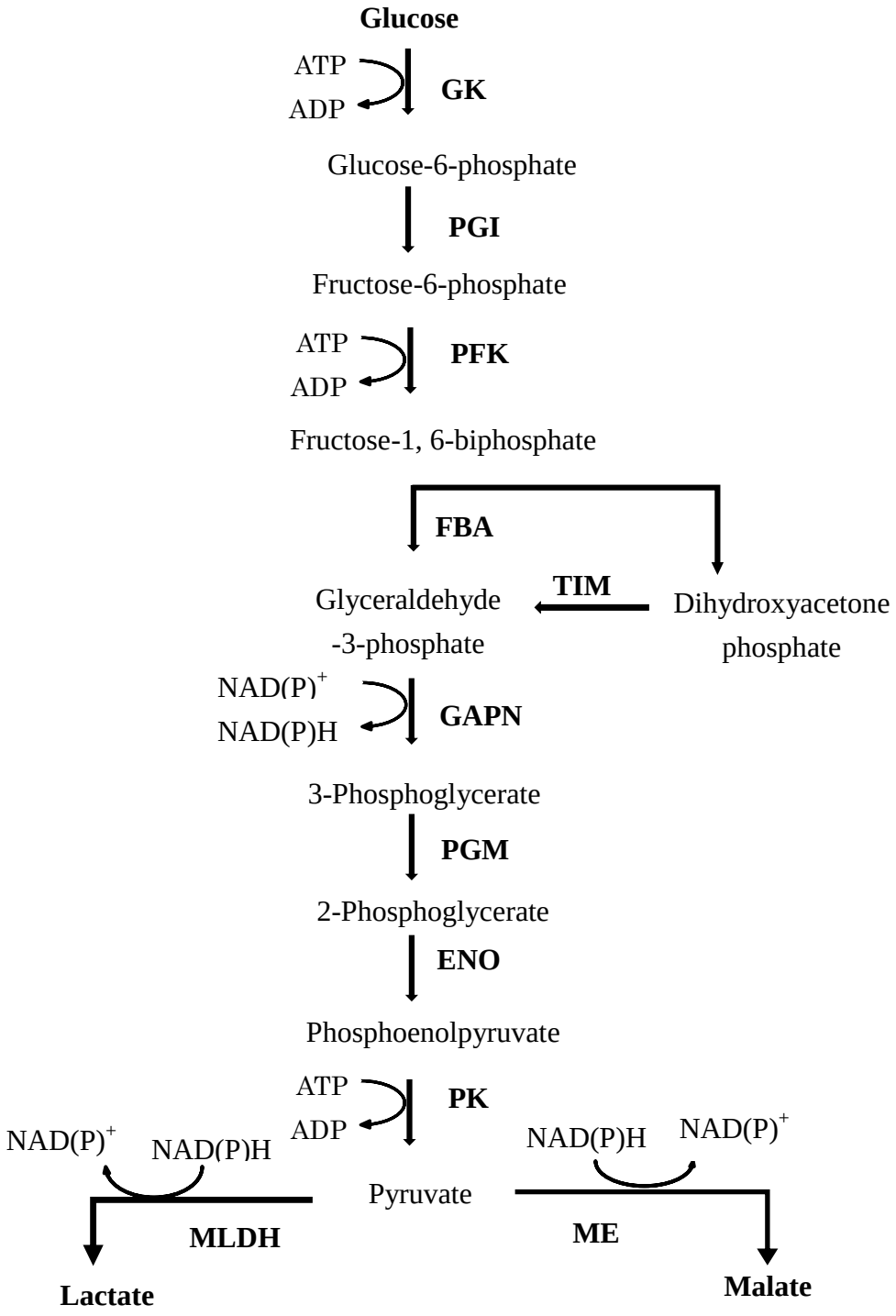

.

Scheme 17: Direct conversion lactate or malate from glucose through the chimeric EM pathway with thermophilic enzymes.

1.4 Objective of this study

Although the *in vitro* metabolic engineering using thermophilic biocatalysts has a number of potential advantages compared to those with mesophilic biocatalysts, there still remains a significant room to improve their feasibility. In this thesis, the author aimed to improve the operational simplicity of thermophilic-enzyme-based *in vitro* metabolic engineering with particular focuses on (1) prevention of the thermolysis of *E. coli* cells and (2) co-expression of multiple thermophilic enzymes in a single recombinant cell.

1.4.1 Thermolysis of *E. coli* cells harboring thermophilic enzymes

The direct use of recombinant *E. coli* having heterologous thermophilic enzymes at high temperature results in the thermolysis of *E. coli* cells and leads to the heat-induced leakage of the thermophilic enzymes. Ren et al. (2007) reported that more than 60% of the thermophilic esterase from a hyperthermophilic archaeon *Aeropyrum pernix* K1 leaked out of the recombinant *E. coli* cells after a heat treatment of the cell suspension at 60^{o}C for 20 min. The heat-induced leakage of thermophilic ATP-dependent glycerol kinase of a hyperthermophile *Thermococcus kodakarensis* (*Tk*GK) was also observed after an incubation of recombinant *E. coli* cells at 70°C for 20 min (Restiawaty et al.,

2011). Although the heat-induced leakage of thermophilic enzymes improves the accessibility between the enzymes and substrates, it impedes the applicability of the thermophilic whole-cell biocatalysts in repeated and continuous reactions, preventing us from exploiting the excellent stability of thermophilic biocatalysts. A possible solution to this problem is the use of cross-linking chemicals to immobilize the enzymes inside the cell membrane structures. In chapter 2, the author deals with the development of a continuous bioconversion system using thermophilic whole-cell biocatalyst. The recombinant *E. coli* cells harboring the thermophilic fumarase from *Thermus thermophilus* were treated with a low concentration of glutaraldehyde (GA) to prevent the heat-induced leakage of the enzyme. The membrane permeability of the GA-treated *E. coli* cells to relatively small molecules was improved by heat treatment whereas the overall structure of the cells was not apparently changed. The GA-treated *E. coli* cells having the thermophilic fumarase were used for the hydration of fumarate to malate in a continuous reactor for more than 600 min with a molar conversion yield of 60% or higher.

1.4.2 Co-expression of multiple thermophilic enzymes in a single *E. coli* cell

In general, a certain number of enzymes have to be separately prepared in different batches for the construction of an *in vitro* metabolic pathway. This prevents us from making full use of one of the most advantageous features of biocatalysts, namely their ability to implement multistep reactions in a single reactor. Co-expression of a series of thermophilic enzymes involved in the designed pathway into a single *E. coli* cell can provide a possible solution to this limitation. By simply heating multiple-gene-expression recombinant *E. coli* cells, denaturation of mesophilic proteins and one-step preparation of the full set of thermophilic enzymes can be achieved.

In chapter 3, genes encoding nine thermophilic enzymes involved in the non-ATP-forming chimeric glycolytic pathway (Ye et al., 2012) were co-expressed in a single recombinant *E. coli* strain by assembling them in an artificial operon. The cell-free extract of the multiple-gene-expression *E. coli* showed higher specific activities of the thermophilic enzymes compared to those in an enzyme cocktail prepared from a mixture of single-gene-expression strains, in each of which one of the nine thermophilic enzymes was overproduced. By heating the crude extract of the multiple-gene-expression cells at 70^{o}C, a full set of glycolytic pathway enzymes was prepared and used for the direct conversion of glucose to pyruvate or lactate.

2. Development of a continuous bioconversion system using a thermophilic whole-cell biocatalyst

2.1 Introduction

Thermophilic enzymes are promising tools for biotransformation owing to their high operational stability, co-solvent compatibility, and low risk of contamination (Persidis, 1998; Turner et al., 2007; Cava et al., 2009). The direct use of recombinant mesophiles (e.g., *Escherichia coli*) having heterologous thermophilic enzymes at high temperatures results in the denaturation of indigenous enzymes and the elimination of undesired side reactions; therefore, highly selective whole-cell catalysts comparable to purified enzymes can be readily prepared. Honda et al. (2010) have demonstrated that a rational combination of such thermophilic whole-cell catalysts enables a construction of *in vitro* artificial biosynthetic pathways for the production of value-added chemicals. More recently, Ye et al. (2012) have successfully constructed a chimeric Embden-Meyerhof pathway with a balanced consumption and regeneration rates of ATP and ADP, using nine recombinant *E. coli* strains, each of which overproduces a thermophilic glycolytic enzyme.

The membrane structure of *E. coli* cells is partially or entirely disrupted at high temperatures, and thus thermophilic enzymes, which are produced as intracellular

soluble proteins, leak out of the cells (Tsuchido et al., 1985; Guiliano et al., 2004; Ren et al., 2007; Restiawaty et al., 2012). Although the heat-induced leakage of thermophilic enzymes results in better accessibility between the enzymes and substrates, it limits the applicability of thermophilic whole-cell catalysts to continuous and repeated-batch reaction systems. This limitation prevents us from exploiting the most advantageous feature of thermophilic biocatalysts, namely, their excellent stability. A potential strategy to overcome this limitation is the integration of thermophilic enzymes to the membrane structure of cells. Restiawaty et al. (2012) reported that the heat-induced leakage of a thermophilic glycerol kinase from recombinant *E. coli* cells could be prevented by fusing the enzyme to an *E. coli* membrane-intrinsic protein, YedZ. However, the specific enzyme activity of the recombinant *E. coli* having the YedZ-fused enzyme decreased to 6% of that of the recombinant with the non-fusion enzyme. A tight integration of the glycerol kinase to the *E. coli* membrane structure might have prohibited the conformational change of the enzyme, resulting in a decreased specific activity. Thus, the screening for a suitable membrane-anchoring protein would be essential to mitigate the loss of the specific activity.

An alternative approach to preventing the heat-induced leakage is the use of protein cross-linking reagents for the consolidation of the cell membrane as well as for

the linkage of enzymes to the membrane structure. In this approach, unlike the integration via membrane-anchoring proteins, cross-linkage level can be readily controlled by changing the conditions for the cross-linking reaction, and thus the best compromise between the prevention of the heat-induced leakage and the maintenance of the specific enzyme activity can be achieved. Glutaraldehyde and related dialdehydes are some of the most effective protein cross-linking reagents and have been widely used for biocatalyst immobilization (Kim et al., 1997; Fernández-Lorente et al., 2006; Singh et al., 2008; Stojkovič et al., 2011). GA is mainly used to immobilize enzymes to carriers such as activated charcoal, anion-exchanging resin, and glass beads. Generally, for the cross-linkage of enzymes to these carriers, the enzyme has to be isolated from cells, purified to a certain level, attached to carriers in a suitable way, and then cross-linked with GA.

In this chapter, *E. coli* cells having a thermophilic fumarase were treated with GA. GA-treated cells were heated at 70^{o}C to inactivate the intrinsic enzymes, and then directly used for the conversion of fumarate to malate. Through this simple procedure, many steps required in conventional procedures for the preparation of immobilized enzymes, such as protein extraction, enzyme purification, and the preparation of immobilizing carriers, could be entirely skipped, and a highly stable and selective

immobilized enzyme, of which heat-killed *E. coli* cells served as carriers, could be prepared.

2.2 Materials and Methods

2.2.1 Bacterial strain and culture conditions

The expression vector for the thermophilic fumarase (*Tt*FTA) was obtained from the RIKEN *Thermus thermophilus* HB8 expression plasmid library (Yokoyama et al., 2000) and designated pET-*Tt*FTA. The expression vector for the malic enzyme of *Thermococcus kodakarensis* KOD1 (*Tk*ME) was constructed as described elsewhere (Ye et al., 2013). *E. coli* Rosetta 2 (DE3) pLysS (Novagen, Madison, WI) was used as the host cell for gene expression. Recombinant *E. coli* was cultured in a 500-mL Erlenmeyer flask containing 200 mL of Luria-Bertani broth supplemented with 100 μg/mL ampicillin and 34 μg/mL chloramphenicol. Cells were cultivated at 37^{o}C with orbital shaking at 180 rpm. Isopropyl β-D-1-thiogalactopyranoside (IPTG) was added to the culture at a final concentration of 0.4 mM in the late-log phase. After 3-h induction, the cells were harvested by centrifugation and washed once with 0.1 M sodium phosphate buffer (pH 7.0).

2.2.2 Glutaraldehyde treatment

Two hundred milligrams of wet cells was suspended in 1 mL of 0.1 M sodium phosphate buffer (pH 7.0). GA solution (25% in water, Nacalai tesque, Kyoto, Japan) was added to the cell suspension to give final concentrations of 0.03-0.15% (vol/vol). The mixture was gently stirred at 4°C for 1 h. The treated cells were harvested by centrifugation at 8,000 × *g* for 10 min and then washed once with the same buffer.

2.2.3 Enzyme assay

*Tt*FTA activity was assessed at 70°C by coupling with the *Thermococcus* malic enzyme, which catalyzes a $NADP^+$-dependent decarboxylation of malate to pyruvate. *E. coli* cells having either *Tt*FTA or *Tk*ME were suspended in 0.1 M sodium phosphate buffer (pH 7.0) and disrupted using an ultrasonicator (UD-201, Kubota, Osaka, Japan) at 40 W for 3 min. The resulting lysate was heated at 70^oC for 20 min. After the removal of cell debris and denatured proteins by centrifugation, the resulting supernatant was used as the enzyme solution. Enzyme activity was measured spectrophotometrically by monitoring the increase in the absorbance of NADPH at 340 nm. A molar absorption coefficient for NADPH of 6.22×10^3 $M^{-1}cm^{-1}$ was used. One unit of enzyme was defined as the amount of enzyme that catalyzes the production of 1μmol of NADPH per

1 min. The standard reaction mixture contained 1.25 mM sodium fumarate, 50 mM $MnCl_2$, 0.1 mM $NADP^+$, 0.1 U *Tk*ME, and 0.1 M phosphate buffer (pH 8.0), in a total volume of 1 mL. The reaction was started by adding an appropriate amount of *Tt*FTA solution. The initial rates of the whole-cell reaction were determined in the same manner by directly using a low concentration of the free or GA-treated cells having *Tt*FTA as catalyst instead of cell-free extract.

For the determination of catalytic performance in malate production using the whole cells, free or GA-treated *E. coli* cells having *Tt*FTA were suspended in 0.1 M phosphate buffer at a concentration of 8 mg (wet weight)/mL. Cells were used as catalysts after the heat treatment at 70^{o}C for 20 min. The reaction was initiated by adding 2.5 mL of the heat-treated cell suspension into a screw-capped vial (3.5 × 6.5 cm) containing 2.5 mL of 0.4 M sodium fumarate in the same buffer, which was preheated at 70^{o}C. The reaction was performed at 70^{o}C with stirring. Aliquots (0.5 mL) of the mixture were withdrawn after the reaction for 5, 10, 30, and 60 min, acidified with HCl to stop the reaction, and then subjected to high-performance liquid chromatography (HPLC).

2.2.4 Heat-induced leakage of *Tt*FTA

The free and GA-treated *E. coli* cells having *Tt*FTA were suspended in 0.1 M phosphate buffer (pH 7.0) at 200 mg (wet weight)/mL and incubated at 70^{o}C. After the incubation for 5, 10, 30, and 60 min, the cells and their debris were removed by centrifugation at 15,000 × *g* for 10 min at 4^{o}C. The supernatants were resubjected to heat treatment at 70^{o}C for 20 min. Denatured proteins were removed by centrifugation, and the *Tt*FTA activity in the supernatant was determined. Leakage level was expressed as the percentage of *Tt*FTA activity in the cell-free extract, prepared by subjecting the same concentration (200 mg/mL) of the free-cell suspension to ultrasonication, followed by heat treatment at 70^{o}C for 20 min.

2.2.5 Electron microscopic analysis

Scanning electron microscopy (SEM, S-5200, Hitachi, Tokyo, Japan) was used to take images of the free and GA-treated *E. coli* cells before and after the heat treatment at 70^{o}C for 20 min. The suspensions of the free and GA-treated cells were centrifuged at 5,000 × *g* for 10 min. The pellets were fixed with 2.5% (w/w) GA in 0.2 M phosphate buffer for 1 h, and then stained with 5% (w/w) osmic acid in the same buffer for 30 min. The samples were dehydrated in a graded ethanol series, lyophilized for 2 h, and then

coated with osmium (HPC-1S hollow cathode plasma CVD, vacuum device, Mito, Japan).

For transmission electron microscopy (TEM), the dehydrated samples were mixed with an epoxy resin solution and then polymerized at 45^{o}C for 5 days. The resin-embedded samples were cut with a glass knife on a Reichert-Nissei ultramicrotome, mounted on carbon-coated copper grids (Nisshin EM, Tokyo), and post-stained with uranyl acetate and lead citrate. TEM was carried out with a JEOL JEM 1200 EX (80 kV) electron microscope.

2.2.6 Effect of heat treatment on the membrane permeability of GA-treated *E. coli* cells

Fluorescein-labeled dextrans with average molecular weights of 3 (Dex3) and 40 kDa (Dex40) (Invitrogen, Carlsbad, CA) were used to evaluate the membrane permeability of the GA-treated cells. The GA-treated cells were suspended in 5 mL of 0.1 M sodium phosphate buffer (pH 7.0) at 200 mg (wet weight)/mL and then heated at 70^{o}C for 20 min. The heated-cell suspension was centrifuged at 8,000 × *g* for 10 min and the cell pellet was washed once with the same buffer. The cells were then resuspended in 5 mL of the buffer containing either Dex3 or Dex40 (0.05 μM each) and incubated in the dark

at room temperature for 30 min with gentle shaking. After incubation, the cells were pelleted by centrifugation at 8,000 × *g* for 10 min and then resuspended in 5 mL of the fresh buffer without dextrans. The resuspended solution was shaken with a vortex mixer for 1 min and then centrifuged at 8,000 × *g* for 10 min. The fluorescence intensity of the supernatant was measured at excitation and emission wavelengths of 494 and 521 nm, respectively. A control experiment was carried out using the GA-treated cells without the heat treatment.

2.2.7 Reusability of GA-treated cells

The reaction mixture containing 4 mg/mL wet cells having *Tt*FTA and 0.2 M sodium fumarate in 0.1 M sodium phosphate buffer (pH 7.0) was placed in a screw-capped cylindrical vessel (ϕ 27 mm) and incubated at 70°C with stirring. After being allowed to react for 30 min, the cells were removed by centrifugation at 8,000 × *g* for 10 min. The supernatant was acidified with HCl, recentrifuged to remove denatured proteins, and then subjected to HPLC to determine the concentrations of malate and fumarate. The reaction was repeatedly performed in the same manner to assess the reusability of the free and GA-treated *E. coli* cells. After each reaction cycle, the cells were harvested by centrifugation at 8,000 × *g* for 10 min, washed with the buffer, and then resuspended in

a fresh reaction mixture.

HPLC was performed using a Shimadzu prominence LC-20 system (Kyoto, Japan) equipped with a COSMOSIL 5C18-AR-II packed column (4.6 x 250 mm, Nacalai Tesque) at 50°C. The UV detector was set at 210 nm, and 0.1% (vol/vol) phosphoric acid solution at a flow rate of 1 mL/min was used as the mobile phase.

2.2.8 Malate production in continuous reactor using GA-treated cells

The reaction mixture (10 mL) comprising 4 mg (wet weight)/mL of the GA-treated cells having *Tt*FTA, 0.2 M sodium fumarate, and 0.1 M sodium phosphate buffer (pH 7.0) was put in a stirred ultrafiltration cell (Model 8010, Millipore, Bedford, MA). A polyvinylidene fluoride membrane filter (ϕ 25 mm; Toray, Kamakura, Japan) (Sawai et al., 2011) was set at the bottom of the reactor to separate cells from the solution. The reaction was performed at 70^{o}C with stirring by a magnetic stirrer. After the reaction for 40 min to achieve a steady state, a fresh substrate solution (0.2 M sodium fumarate in the same buffer) was fed and the product solution was removed using peristaltic pumps (Model 3385, Fisher Scientific, Fair Lawn, NJ). To determine product yield, aliquots (0.1 mL) of the eluent were taken at 40 min intervals and subjected to HPLC. The feeding and removal rates of the solution were maintained at 0.25 mL/min. Residence

time and conversion rate were calculated as follows:

Conversion rate γ (mmol/l/min)

$(S_{in} - S) = \tau \times \gamma$

Residence time τ (min)

$\tau = V / F$

where S_{in} = substrate concentration in the feeding solution, S = substrate concentration in the reactor, F = flow rate, and V = total volume of reaction mixture.

2.3 Results

2.3.1 Effects of GA treatment on heat induced leakage of *Tt*FTA

Figure 2.1 shows the time course of the heat-induced leakage of *Tt*FTA from the recombinant *E. coli* cells. When the free cells were incubated at 70^{o}C, more than 80% of the activity was released out of the cells by 5 min. This observation was in good agreement with previous reports on the thermolysis of *E. coli* cells (Tsuchido et al., 1985; Ren et al., 2007; Restiawaty et al., 2012). Owing to thermolysis, the boundary surface between the supernatant and the pelleted free cells was unclear after the centrifugation at 15,000 × *g* for 10 min. However, the heated GA-treated cells could be clearly separated by centrifugation. The level of *Tt*FTA leakage from the GA-treated cells was considerably lower than that from the free cells and obviously decreased with increasing GA concentration used for the cross-linkage. The leakage from the cells pretreated with 0.11% (vol/vol) or higher GA concentrations was kept under a detectable level after the incubation at 70^{o}C for at least 60 min. However, it was also possible that the decrease in the apparent level of enzyme leakage arose from the inhibitory effect of GA on the enzyme as well as the lowered substrate permeability due to anywhere else the consolidation of the membrane structure caused by the cross-linkage.

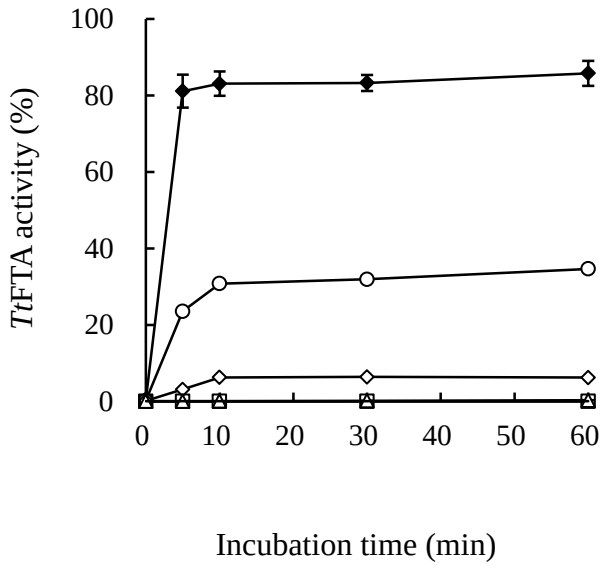

Figure 2.1 Heat-induced leakage of *Tt*FTA from free cells (filled diamonds) and cells pretreated with 0.03 (circles), 0.07 (open diamonds), 0.11 (triangles), and 0.15% (squares) GA. Leakage level was expressed as the percentage of the *Tt*FTA activity in the cell-free extract prepared by ultrasonication. The data are shown as averages ± standard deviations (n = 3).

The author then assessed the catalytic performance of the free and GA-treated cells. As predicted, the catalytic performance of GA-treated cells decreased in proportion to the GA concentration used for their preparation. The initial reaction rates catalyzed by the cells pretreated with 0.03, 0.07, 0.11, and 0.15% of GA were 38, 16, 10, and 6.5% of that obtained using the free cells, respectively (Fig. 2.2A). However, their

abilities for catalyzing fumarate hydration showed no significant difference in product concentration after the reaction for 30 min (Fig. 2.2B). On the basis of these observations, I hereafter employed a GA concentration of 0.11% for the cross-linkage as the best compromise between the prevention of heat-induced leakage and the maintenance of enzyme activity. The conversion of fumarate to malate is a reversible reaction with the equilibrium at approximately 80 mol% (Presečki et al., 2007; Stojkovič et al., 2011) under the standard state (25^{o}C). In this study, the conversion yield using the series of *E. coli* cells having *Tt*FTA reached about 70 mol% after 30 min and then remained constant, regardless of the difference in their specific activities. This indicates that the equilibrium of the reaction under the experimental conditions was achieved at a conversion yield of approximately 70 mol%.

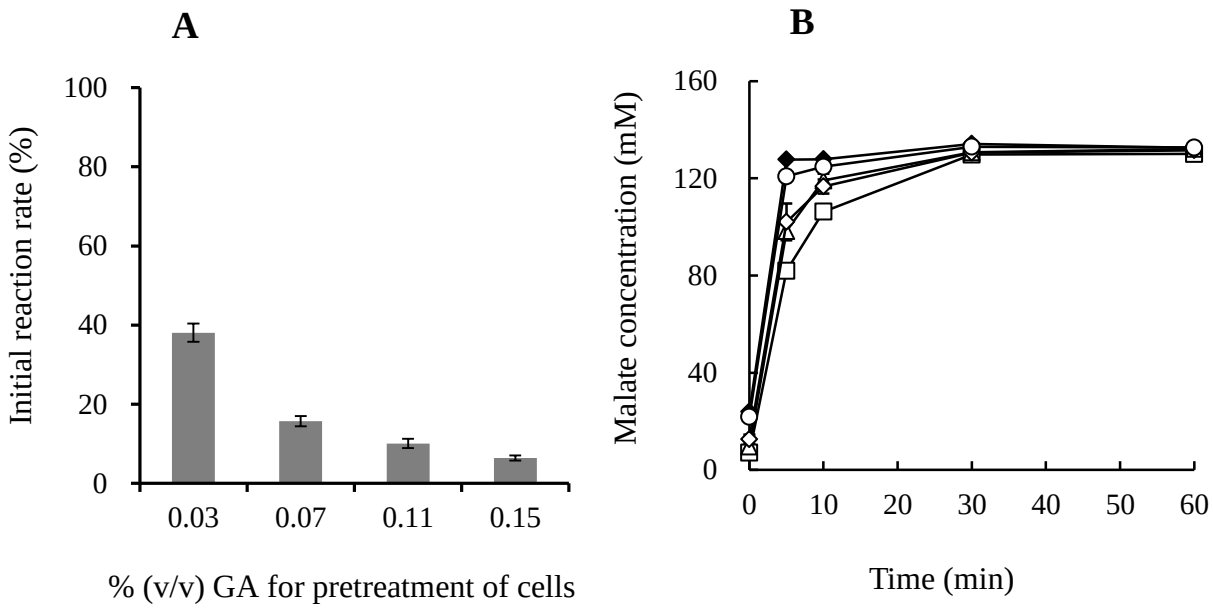

Fig. 2.2 (A) Initial reaction rate obtained using GA-treated cells. The reaction rate of GA-treated cells was expressed as the percentage of the *Tt*FTA activity in the free cells. The data are shown as averages ± standard deviations (n = 3). (B) Time course of malate production catalyzed by free cells (filled diamonds) and cells pretreated with 0.03 (circles), 0.07 (open diamonds), 0.11 (triangles), and 0.15% (squares) GA. The data are shown as averages ± standard deviations (n = 3).

2.3.2 Electron microscopic analysis.

The free and GA-treated cells before heat treatment showed the appearance of normal healthy cells in both SEM and TEM (Fig. 2.3A, C, E, and G). By contrast, after 20-min incubation at 70^{o}C, the SEM image of the free cells displayed cellular structure

disintegration (Fig. 2.3B). Blebs with various sizes were formed on the cell surface. The TEM of the heat-treated free cells showed the surface subsidence of the cells, probably resulting from membrane disruption followed by the leakage of intracellular components, suggesting that the heat-induced leakage of the enzyme was attributed to the collapse of the membrane structure of the cells (Fig. 2.3F).

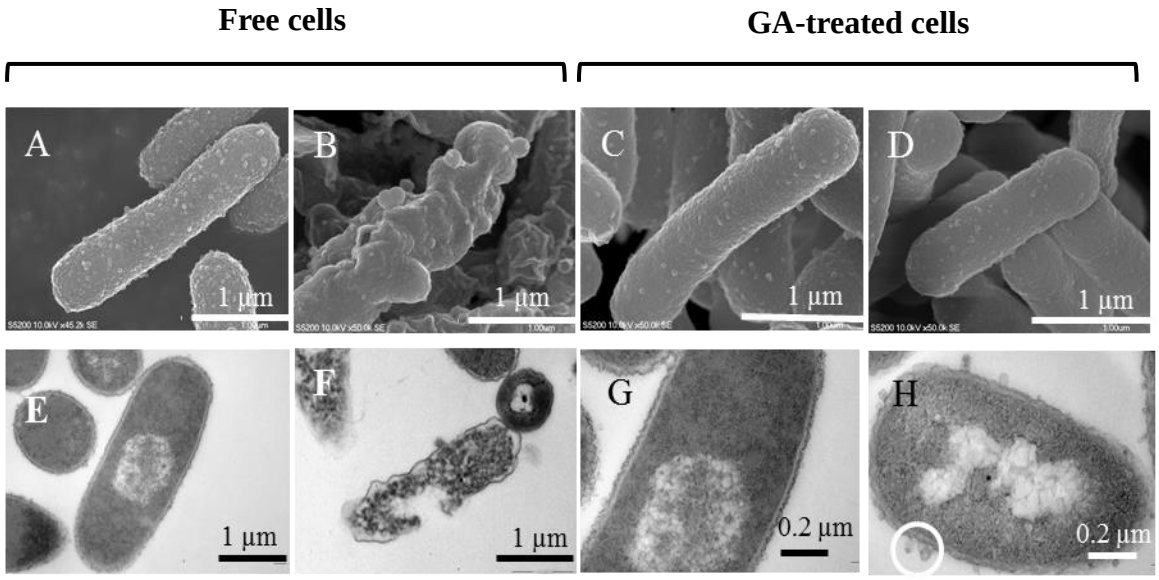

Fig. 2.3 SEM (A-D) and TEM (E-H) images of free and GA-treated *E. coli* cells before (A, C, E, G) and after (B, D, F, H) heat treatment at 70^{o}C for 20 min. The open circle shows small blebs on the cell surface.

In contrast, the overall structure of the GA-treated cells still remained in good condition after the incubation at 70^{o}C for 20 min. Both TEM and SEM showed the

appearance of a cell surface comparable to the surface of healthy cells, except for the formation of some small blebs on the membrane (Fig. 2.3H). This observation supported the notion that the prevention of the heat-induced leakage of *Tt*FTA from *E. coli* cells was, at least in part, attributed to the consolidation of the membrane structure by the GA treatment.

2.3.3 Membrane permeability of GA-treated cells.

Dextrans, polymers of glucose, are hydrophilic polysaccharides characterized by a high molecular weight and good water solubility. Dextran with molecular weights higher than 2 kDa generally cannot permeate into intact cells (Decad et al., 1976). In this study, fluorescein-labeled dextrans with different average molecular weights were used to assess the membrane permeability of the GA-treated cells. The cells were first suspended in a fluorescence-labeled dextran solution, and pelleted by centrifugation, and then the pellet was resuspended in a dextran-free buffer. The fluorescence intensity of the supernatant of the resulting cell suspension correlates with the amount of dextran involved in the cell pellet; therefore, a higher intensity can be obtained when dextran could penetrate into the cell. The slight fluorescence observed in the control experiments with the non-heat-treated cells was likely attributed to the dextran

remaining in the intercellular space of the cell pellets (Fig. 2.4, gray bars).

The fluorescence intensity of the supernatant of the heat-treated cell suspension was almost double that of the non-heat-treated cell suspension when Dex3 was used as an indicator of membrane permeability. On the other hand, when Dex40 was used, no significant difference was observed between the fluorescence intensities of the heat-treated and non-heat-treated cell suspensions. Taken together with the results of electron microscopic observation, these results indicated that the membrane structure of the GA-treated cells was partly disrupted by the heat treatment, while maintaining the overall cell structure; therefore, only relatively small molecules (up to at least 3 kDa) could permeate into and out of the cells.

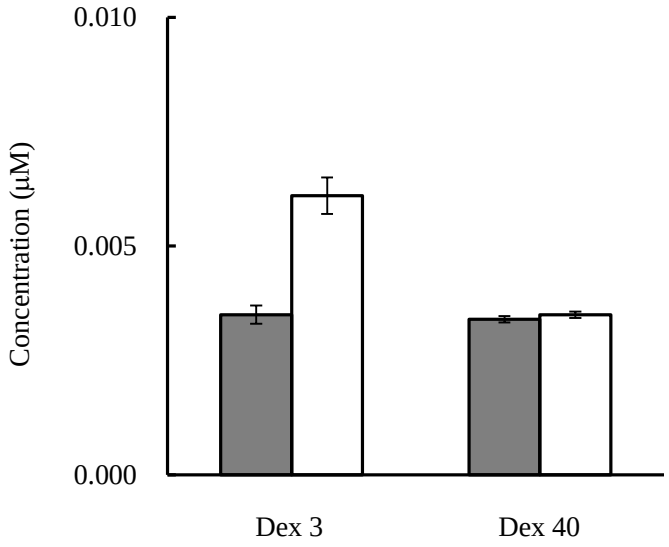

Fig. 2.4 Membrane permeabilities of GA-treated cells with (white) and without (grey) heat treatment. Dextran concentration was determined using a calibration curve obtained by measuring the fluorescence intensities of the serial dilutions of the standards. The data are shown as averages ± standard deviations (n = 3)

2.3.4 Reusability of GA-treated cells in repeated batch reactions.

To evaluate the reusability of the GA-treated cells having *Tt*FTA, batch reactions were repeatedly performed. As a control experiment, the reactions were also carried out using the free cells. Although a slight decrease was observed in product concentration probably due to the thermal inactivation of *Tt*FTA, the product yields of the reactions with the GA-treated cells were maintained above 60 mol% when the reactions were repeated 6 times (Fig. 2.5). By contrast, the product yields with the free cells linearly

decreased with repeated reactions. These results clearly demonstrated the superiority of the GA-treated cells in the repeated reactions.

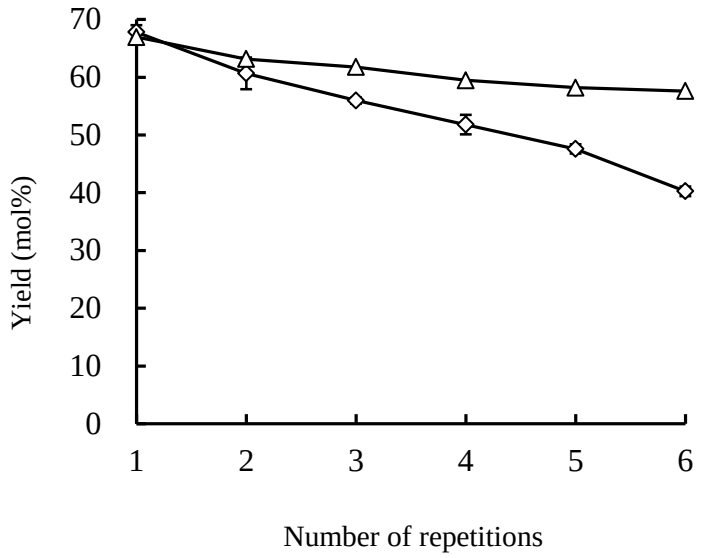

Fig. 2.5 Reusabilities of free (diamonds) and GA-treated (triangles) cells. Each reaction was performed at 70^{o}C for 30 min. The data are shown as averages ± standard deviations (n = 3).

2.3.5 Continuous bioconversion using GA-treated cells as whole-cell catalysts.

For further demonstration of the applicability of the GA-treated cells to long-term bioconversion, the cells were used as a catalyst in a continuous reactor. The reaction rate of fumarate to malate was determined in the batch reaction consisting 120 mM malate and 80 mM fumarate (60% conversion yield) in order to reach to the reaction equilibrium. The residence time (τ) was calculated to be 40 min and the feeding rate of

the substrate solution (0.25 mL/min) was determined. When the free cells were used as a catalyst, the filterability of the separation membrane was significantly impaired, and product recovery at a constant rate could not be achieved (data not shown). This was likely due to the formation of a cake layer on the separation membrane by debris of heat-damaged cells. On the other hand, when the GA-treated cells were used, a continuous product recovery could be maintained for at least 640 min. The production yield decreased slightly in the first 80 min but then remained stable until the end of the operation (Fig 2.6). As a result, an overall product yield of 60 mol% could be achieved during the operation for 640 min. Production rate was 3.0 mmol/L/min, and 19.2 mmol (2.57 g) of malate could be produced from 32 mmol (3.71 g) of fumarate.

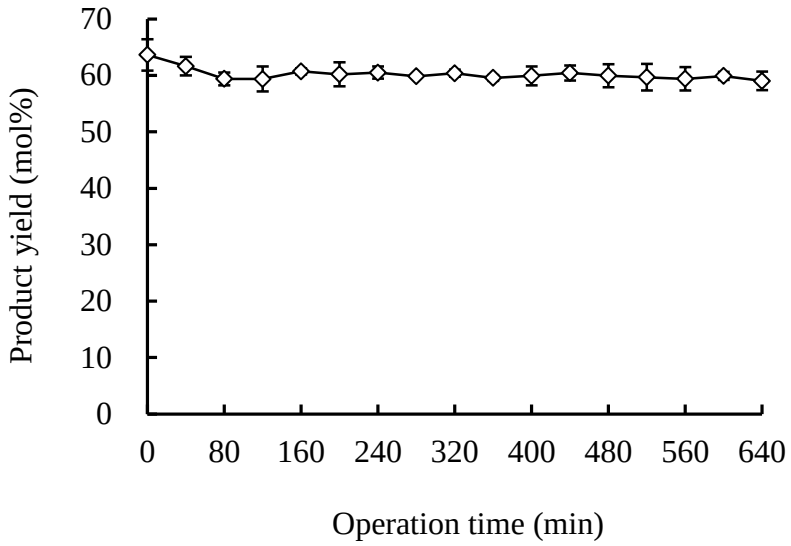

Fig. 2.6 Time course of continuous reaction with GA-treated cells. The data are shown as averages ± standard deviations (n = 3).

2.4 Discussion

In this study, the author demonstrated that the heat-induced leakage of a thermophilic enzyme from recombinant *E. coli* cells could be prevented by the pretreatment of the cells with GA. Through the optimization of GA concentration, a thermotolerant whole-cell catalyst with an acceptable catalytic ability could be prepared and successfully used for a continuous bioconversion of fumarate to malate. This approach is much simpler and more universal for the preparation of stable and selective immobilized enzymes than conventional procedures, which typically involve many

steps, such as protein extraction, enzyme purification, and the preparation of immobilization carriers. The GA-treated cells exhibited sufficient catalytic stability and reusability in both repeated-batch and continuous bioconversions at 70^{o}C. They could catalyze fumarate hydration in the continuous bioreactor over 10 h with a constant product yield of 60 mol% or higher. This productivity was considerably better than that in a previous report on the continuous conversion of fumarate using permeabilized *Saccharomyces* cells, in which the malate yield was about 50% and the enzyme lost 30-50% of its activity after 10 h (Presečki et al., 2009).

The electron microscopic observation of the GA-treated cells revealed that heat treatment caused no apparent change in the overall structure of the cells except for the formation of some small blebs on their surface. GA is a five-carbon dialdehyde that can react with several functional groups of proteins, such as amine, thiol, phenol, and imidazole, and form covalent bonds with them (Habeeb et al., 1968; Nimni et al., 1987; Okuda et al., 1991; Migneault et al., 2004). The GA-mediated stabilization of the membrane structure implied that GA might cross-link between protein molecules in the outer membrane and those in the peptidoglycan layer of the *E. coli* membrane to make it more rigid. In fact, the cells changed to pink-red after the GA treatment; this phenomenon is typically observed as a result of the interaction between membrane

proteins and GA (Munton et al., 1970; McGucken et al., 1973).

The natural barrier function of the cellular membrane often hampers sufficient whole-cell bioconversion since it limits the accessibility of substrates to intracellular enzymes (Chen, 2007). Although no significant change was observed in the overall structure of cells, the membrane permeability test with different sizes of fluorescent-labeled dextrans revealed that relatively small molecules (up to at least 3 kDa) could penetrate through the membrane barrier of the GA-treated cells heated at 70^{o}C. The formation of small blebs observed in the TEM analysis of the heated GA-treated cells was likely responsible for the increased membrane permeability. Most lipids and lipopolysaccharides comprising the cell membrane cannot be fully cross-linked to each other by GA (Migneault et al., 2004). Thus, their orientation might be disrupted at high temperatures. Consequently, small blebs were formed on the membrane of the GA-treated cells, and the rupture of the blebs likely result in the formation of membrane pores, through which molecules having low and middle molecular weights can diffuse. The fact that the dextran with an average molecular weight of 40 kDa hardly penetrated through the membrane was in good agreement with the observation that the leakage of *Tt*FTA (approximately 51 kDa) could be prohibited by GA treatment.

The observation that the GA-mediated consolidation of the membrane structure was involved in the prevention of the heat-induced leakage of the enzyme raised the issue of whether the intracellular enzyme can freely diffuse in the cytosol of the GA-treated cells. To address this question, we attempted to extract the soluble form of *Tt*FTA from the GA-treated cells by disrupting the cells by lysozyme digestion followed by ultrasonication. The *Tt*FTA activity recovered in the resulting lysate was approximately 17% of that detected in the cell-free extract of the free cells (data not shown), indicating that intracellular *Tt*FTA was, at least in part, present in soluble form and freely diffused in the cytosolic fraction.

2.5 Summary

In this chapter, the continuous bioconversion system using thermophilic whole-cell biocatalyst has been developed. *Escherichia coli* cells having the thermophilic fumarase from *Thermus thermophilus* (*Tt*FTA) were treated with glutaraldehyde to prevent the heat-induced leakage of the enzyme, and the resulting cells were used as a whole-cell catalyst in continuous bioconversion of fumarate to malate. Interestingly, although electron microscopic observations revealed that the cellular structure of glutaraldehyde-treated *E. coli* was not apparently changed by the heat treatment, the membrane permeability of the heated cells to relatively small molecules (up to at least 3 kDa) was significantly improved. By applying the glutaraldehyde-treated *E. coli* having

*Tt*FTA to a continuous reactor equipped with a cell-separation membrane filter, the enzymatic hydration of fumarate to malate could be operated for more than 600 min with a molar conversion yield of 60% or higher.

3. Assembly and multiple gene expression of thermophilic enzymes in *Escherichia coli* for *in vitro* metabolic engineering

3.1 Introduction

Fermentation-based production of industrial chemicals offers distinct advantages over organic synthesis, such as the selective production of chemically indistinguishable isomers and the use of biomass, which is a highly complex mixture of biomolecules, as a starting material. In addition, multistep reactions can be operated in a single reactor and thus step-by-step purifications of the reaction intermediates can be omitted (Burda et al., 2008). These advantages of fermentation-based processes are conferred mostly by the excellent selectivity of enzymes. The emergence of metabolic engineering approaches has expanded the applicability of fermentation-based processes to the production of a wider range of industrial chemicals, involving fuels (Atsumi et al., 2008; Choi et al., 2013), commodity chemicals (Nakamura et al., 2003; Whited et al., 2010), and pharmaceuticals (Ajikumar et al., 2010; Paddon et al., 2013).

However, installation of an artificially engineered pathway in living organisms often leads to competition with natural metabolic pathways for intermediates and cofactors, resulting in insufficient yield of the product of interest. One of the possible strategies to overcome this limitation is to avoid using living microorganisms and using only enzymes involved in the synthetic pathway. Recently, a variety of *in vitro* artificial metabolic pathways have been designed and constructed for the production of alcohols (Guterl et al., 2012; Krutsakorn et al., 2013), organic acids (Ye et al., 2012; Ye et al., 2013), carbohydrates (You et al., 2013), hydrogen (Woodward et al., 2000; Zhang et al., 2007), and even electricity (Zhu et al., 2014). Implementation of complex biochemical reactions by *in vitro* assembly of multiple metabolic enzymes has several potential

advantages, such as elimination of by-product formation, thermodynamic prediction of product yield, and simplification of downstream processes for product recovery (Ye et al., 2012). However, despite these potential advantages, there is still significant room for improvement in *in vitro* metabolic engineering approaches. As described in chapter 1, Rollin et al. (2013) pointed out that there remain four key challenges to be overcome for the commercial application of *in vitro* metabolic engineering. In addition to these points, the enzymes required for the construction of an *in vitro* artificial metabolic pathway have to be separately prepared in different batches, preventing full exploitation of one of the most advantageous features of biocatalytic conversions, namely their ability to implement multistep reactions in a single reactor.

Possible solutions to some of these problems can be provided by employing thermophilic enzymes as the catalytic modules for the pathway construction. Heat-treatment of recombinant mesophiles (*e.g.*, *Escherichia coli*) in which a set of thermophilic enzymes comprising the pathway of interest are overproduced, results in the denaturation of indigenous enzymes and one-step preparation of a cocktail of recombinant thermophilic enzymes. In addition, the high operational stability of thermophilic enzymes can mitigate the major disadvantage of *in vitro* enzymatic conversions, the inability of protein synthesis and renewal. In the present, genes encoding nine thermophilic enzymes, which are involved in a non-ATP-forming chimeric glycolytic pathway (Ye et al., 2012), were assembled in an artificial operon and co-expressed in a single recombinant *E. coli* strain. Coupling the heat-treated crude extract of the resulting recombinant *E. coli* with other thermophilic enzymes including the H_2O-forming NADH oxidase or the malate/lactate dehydrogenase facilitated one-pot conversion of glucose to pyruvate or lactate, respectively.

3.2 Materials and Methods

3.2.1 Bacterial strains

E. coli DH5α was used for general molecular cloning and gene expression. *Bacillus subtilis* BUSY9797 (Hiroe et al., 2012), which can repress expression from the Pr promoter, was used for gene assembly. Both *E. coli* and *B. subtilis* were cultivated in Luria-Bertani (LB) medium at 37°C. Ampicillin (100 μg/mL), chloramphenicol (12.5μg/mL) and tetracycline (10 μg/mL) were used for the selection of recombinant strains. The temperature-inducible Pr/CI857 system (Jechlinger et al., 1999) was employed for the expression of heterologous genes in *E. coli* because the use of another promoter results in the unregulated expression of heterologous genes in *B. subtilis* and tends to interfere with the gene assembly (Nishizaki et al., 2007). Gene expression in *E. coli* was induced by shifting the cultivation temperature to 42°C at the late log phase. Further, cells were cultivated at 42°C for 4 h and then harvested by centrifugation.

3.2.2 Plasmid construction

The *E. coli-B. subtilis* shuttle vector, pGETS118 (Kaneko et al., 2005), and a series of pUC19 destination vectors with unique *Dra*III restriction sites (Hiroe et al., 2012) were gifts from K. Tsuge (Keio University, Japan).

The pRCI vector, which harbors the Pr promoter and an expression cassette for the *cI857* repressor of λ phage, was constructed as described as follow. The *lacI* promoter was amplified by PCR from pET21a (Novagen, Madison, WI) using following primers: lacI-F, 5′-GCGGATCCGAATTCAAGGGAGAGCGTCGAGATCC-3′ (*Bam*HI and *Eco*RI restriction sites are underlined) and lacI-R, 5′-GGTTTCTTTTTTGTGCTCATATTCACCACCCTGAATTGACTC-3′. The gene

encoding the *cI857* repressor was amplified using λ DNA (Toyobo, Osaka, Japan) as the template. The oligonucleotide primers of cI857-F (5′-ATGAGCACAAAAAAGAAA-CCATTAACACAA-3′) and cI857-R (5′-GGAGCGGCCGCTTACTATGTTATGTTC-TGAGGGGAGTGAAA-3′, *Not*I restriction site is underlined) were used for the amplification. The PCR products were mixed and used as the template for overlapping PCR to construct the expression cassette of the *cI857* repressor. The primer pair of lacI-F and cI857-R was used for the overlapping PCR. The amplicon was digested with *Not*I and *Bam*HI.

A 2,670-kb internal fragment of pBR322 (Toyobo) containing the ColE1 ori and the ampicillin resistance gene was amplified by PCR with the following primers: pBR-F, 5′-GGAGCGGCCGCGCTACCCTGTGGAACACCTACAT-3′ (*Not*I restriction is underlined), and pBR-R, 5′-CGCGGATCCTTCTTGAAGACGAAAGGGCCTC-3′ (*Bam*HI restriction site is underlined). The PCR product was digested with *Not*I and *Bam*HI, and ligated with the expression cassette of the *cI857* repressor, and the resulting plasmid was designated as pBR-CI857.

Further, the Pr promoter was amplified from λ DNA using the following primers: PR-F, 5′-GGAAGATCTACGTTAAATCTATCACCGCAAGGGATAAATATTTAACA-CCGTG-3′ (*Bgl*II restriction sites are underlined), and PR-R, 5′-CCGCTC-GAGGCTCTTCACACCATACAACCTCCTTAGTACATGCAAC-3′ (*Xho*I and *Bsp*QI restriction sites are underlined). The T7 terminator region of pET21a was amplified using T7T-F (5′-CCGCTCGAGGCTCTTCATAAGGCTGCTAACAAAGC-3′, *Xho*I and *Bsp*QI restriction sites are underlined) and T7T-R (5′-GGAGAATTC-ATCCGGATATAGTTCCTCCTTTCAG-3′, *Eco*RI restriction site is underlined) primers. The PCR-amplified Pr promoter and T7 terminator were digested with *Xho*I and then

tandemly ligated with T4 DNA ligase (Toyobo). The ligation product was further amplified by PCR using the primer pair of PR-F and T7T-R. The amplified DNA was digested with *Bgl*II and *Eco*RI and then introduced into the corresponding sites of pBR-CI857. Finally, a point mutation was introduced into the resulting plasmid to eliminate the extra-*Bsp*QI restriction site derived from pBR322, using the PrimeStar mutagenesis kit (Takara Bio, Ohtsu, Japan) with the primer pair of MUT-1, 5′-TCAGGCGCTATTCCGCTTC-3′ and MUT-2, 5′-GAAGCGGAATAGCGCCT-GA-3′ (the mutated nucleotide is underlined).

The expression vector of NADH oxidase was constructed as followed description. The codon-optimized gene encoding NADH oxidase from *Thermococcus profundus* was synthesized and expressed in *E. coli*. The synthetic gene was flanked with *Nde*I and *EcoR*I restriction sites at its 5'- and 3'-terminals, respectively. The gene was digested with these restriction enzymes and introduced into the corresponding sites of pET21a. *E. coli* BL21 (DE3) (Novagen) was used as a host for gene expression.

3.2.3 Gene assembly

Codon-optimized genes that encode glucokinase (GK), glucose-6-phosphate isomerase (PGI), 6-phosphofructokinase (PFK), fructose-bisphosphate aldolase (FBA), triosephosphate isomerase (TIM), enolase (ENO), and pyruvate kinase (PK) of *Thermus thermophilus* HB8, non-phosphorylating glyceraldehyde-3-phosphate dehydrogenase (GAPN) of *Thermococcus kodakarensis* KOD1, and cofactor-independent phosphoglycerate mutase (PGM) of *Pyrococcus horikoshii* OT3, were assembled into

an artificial operon by the ordered gene assembly in *B. subtilis* (OGAB) method (Tsuge et al., 2003). The 5′-untranslated region (UTR) sequence containing the ribosome binding site (RBS) of pET21a was associated upstream of the start codon of each synthetic gene. Both 5′- and 3′-ends of the synthetic genes were flanked by *Bsp*QI restriction sites. Genes were digested with *Bsp*QI and introduced to the corresponding sites of the series of pUC destination vectors. The resulting plasmids (pUC19V-1st-GAPN, pUC19V-2nd-FBA, pUC19V-3rd-GK, pUC19V-4th-ENO, pUC19V-5th-PGM, pUC19V-6th-PFK, pUC19V-7th-PK, pUC19V-8th-TIM, and pUC19V-9th-PGI) were digested with *Dra*III to generate unique 3-base cohesive ends required for gene ordering. Digested DNA fragments were gel-purified, mixed at an appropriate concentration (2 fmol/mL each), and ligated to the *Sfi*I restriction site of pGETS118 with T4 DNA ligase (Toyobo). Transformation of *B. subtilis* was performed as described by Tsuge et al. (2003). In addition, the plasmid harboring the assembled genes was isolated from the resulting transformant and designated as pGETS-CGP, and *E. coli* DH5α was co-transformed with pGETS-CGP and pRCI by electroporation. The nucleotide sequence of the constructed operon is shown in Supplementary Fig S1.

3.2.4 Real-time PCR

The mRNA transcription levels were determined by real-time PCR (RT-PCR). Total RNA was extracted using the RNeasy Mini kit (QIAGEN, Valencia, CA), and then subjected to reverse transcription using the ReverTra Ace qPCR RT kit (Toyobo). RT-PCR was performed with the StepOnePlus real-time PCR system (Applied Biosystems, Foster City, CA) using SYBR green real-time PCR Master Mix-plus (Toyobo). Standard curves were generated for estimating mRNA levels by linear

regression analysis. The expression levels of the heterologous genes were normalized to that of *rrsA* (16s rRNA) as a reference gene. Primers used for RT-PCR analysis are shown in Table 3.1.

Table 3.1 Primers used for RT-PCR

Name	Sequence (5'→3')	Name	Sequence (5'→3')
GK-F	ACTAAGATCGCAGCTGGTGTGTT	GAPN-F	AATCTTTGAGGGCATTTTCCG
GK-R	CACCTGCTTCACGCTCTGC	GAPN-R	GCAATCAGGCTACCGTCGAT
PGI-F	TTGAAGACTTCGTTCTGATCGGTA	PGM-F	CCGATCAAAGAACTGAACGGTC
PGI-R	GCTCCGGCTCAACGTGAT	PGM-R	CTGACCCGGCTTAATCGGA
PFK-F	TGGGTGTGGAAGTTATTGGTATCC	ENO-F	GGTTTCCCGACTGTTGAAGC
PFK-R	CACCGCGCTGAATGATGTT	ENO-R	TCACGCAGCTCCAGTGCTT
FBA-F	CTGAAAGCAGACATTGGTAGCG	PK-F	ATGTTTTCCGCCTGAACTTCTC
FBA-R	ATCGTCACCGATGTGGAAAAC	PK-R	CCTGCAGCACAGCCAGAGT
TIM-F	AAGCACGTGTTTGGTTTGCTG	rrsA-F	AGTCCACGCCGTAAACGATGT
TIM-R	ACCGTAACCAACCTGGGTTTC	rrsA-R	TTTAACCTTGCGGCCGTACTC

3.2.5 Enzyme assay

The recombinant *E. coli* producing thermophilic enzymes was suspended in 50 mM HEPES-NaOH buffer (pH 7.0) and disrupted with a UD-201 ultrasonicator (Kubota, Osaka, Japan). The crude lysate was heated at 70°C for 30 min and centrifuged to remove cell debris and denatured proteins, and the supernatant was used as an enzyme solution.

The enzyme assay was performed as described previously (Ye et al., 2012). Briefly, an appropriate amount of GK was incubated in a mixture that contained 50 mM HEPES-NaOH buffer (pH 7.0), 0.2 mM ATP, 5 mM $MgCl_2$, 0.5 mM $MnCl_2$, 1 mM NAD^+, 0.1 mM glucose-1-phosphate, and an excess amount of PGI, PFK, FBA, TIM, and GAPN. The mixture was pre-incubated for 2 min at 70°C, and then the reaction was initiated by adding 0.1 mM glucose. Further, the reduction of NAD^+ was monitored at 340 nm using a UV-VIS spectrophotometer (Model UV-2450, Shimadzu, Kyoto, Japan). Similarly, the activities of PGI, PFK, FBA, TIM, and GAPN were spectrophotometrically evaluated in the mixture containing the substrate for each enzyme (0.1 mM of glucose-6-phosphate, fructose-6-phosphate, fructose-1,6-bisphosphate, dihydroxyacetone phosphate, or 0.2 mM glyceraldehyde-3-phosphate, respectively) instead of glucose. The activity of PGM was determined by coupling with ENO, PK, and *Thermus thermophilus* lactate dehydrogenase (*Tt*LDH). The reaction mixture contained 0.2 mM ADP, 5 mM $MgCl_2$, 0.5 mM $MnCl_2$, 0.2 mM NADH, and an excess amount of ENO, PK, and *Tt*LDH. After preincubation at 70°C for 2 min, the reaction was initiated by the addition of 0.2 mM 3-phosphoglycerate and the consumption of NADH was monitored at 340 nm. ENO and PK activity was determined in the same manner using 0.2 mM 2-phosphoglycerate and

phosphoenolpyruvate, respectively, as substrates. One unit of an enzyme was defined as the amount consuming 1 μmol of substrate per min under the assay conditions.

The NADH oxidase assay was performed as follow. The recombinant *E. coli* was cultivated at 37^{o}C in LB medium supplemented with 100 μg/mL ampicillin. Gene expression was induced by the addition of 0.2 mM isopropyl β-D-1-thiogalactopyranoside (IPTG) at the late-log phase. Cells were harvested by centrifugation, suspended in 50 mM HEPES-NaOH (pH 7.0), and disrupted by ultrasonication. The crude lysate was heated at 70^{o}C for 30 min, and centrifuged to remove the debris and denatured proteins. The resulting supernatant was used as the enzyme solution.

The enzyme activity was determined by monitoring the oxidation of NADH at 340 nm. The reaction mixture comprising of 50 mM HEPES-NaOH (pH 7.0), 5 mM $MgCl_2$, 0.5 mM $MnCl_2$, 0.02 mM flavin adenine dinucleotide, 0.2 mM NADH was preincubated at 70^{o}C for 2 min and then the reaction was started by the addition of appropriate amount of enzyme.

3.2.6 Determination of pyruvate production rate

Wet cells of the recombinant *E. coli* harboring pGETS-CGP and pRCI were suspended in 50 mM HEPES-NaOH buffer (pH 7.0) at a concentration of 50 mg mL^{-1} and disrupted by ultrasonication. The crude extract was heated at 70°C for 30 min and then

directly used as a catalyst without removing cell debris and denatured proteins. Alternatively, the crude extract was prepared from the mixture of the recombinant strains, in each of which a single one of the nine thermophilic enzymes was overproduced using the pRCI vector. The recombinant strains producing GK, PGI, PFK, FBA, TIM, GAPN, PGM, ENO, and PK were mixed at concentrations of 5, 1, 2, 5, 1, 32, 2, 1, and 1 mg wet cells mL^{-1}, respectively, disrupted by ultrasonication, and then heated at 70°C for 30 min.

The reaction mixture (1 mL) contained 50 mM HEPES-NaOH buffer (pH 7.0), 0.1 mM glucose, 5 mM $MgCl_2$, 0.5 mM $MnCl_2$, 0.2 mM ATP, 0.2 mM ADP, 1 mM NAD^+, 1 mM glucose-1-phosphate, and the heat-treated crude extract prepared from 50 mg wet cells. NADH oxidase from *Thermococcus profundus* was added to the reaction mixture at 0.1 U mL^{-1} for NAD^+ regeneration. The reaction was performed at 70°C with mixing (1,400 rpm) using a thermomixer (Eppendorf, Hamburg, Germany). After incubation for 10 min, the reaction was stopped by the addition of 0.8 mL of 1 M HCl dissolved in ice-cold methanol. Further, the denatured proteins were removed by centrifugation, and the mixture was ultrafiltered using Amicon 3 K (Millipore). The filtrate was mixed with an equal volume of 1 mg mL^{-1} *o*-phenylenediamine in 3 M HCl (Mühling et al., 2003) for a fluorescence label of pyruvate. The mixture was incubated at 80°C for 60 min and then analyzed by high-performance liquid chromatography (HPLC).

3.2.7 Lactate production

The reaction mixture (4 mL) contained 50 mM HEPES-NaOH buffer (pH 7.0), 0.1 mM glucose, 5 mM $MgCl_2$, 0.5 mM $MnCl_2$, 0.2 mM ATP, 0.2 mM ADP, 1 mM NAD^+, 0.2 mM NADH, 0.2 mM 3-phosphoglycerate, 0.2 mM pyruvate and 1 mM

glucose-1-phosphate. The heat-treated crude extract, which was prepared from 200 mg wet cells of *E. coli* harboring pGETS-CGP and pRCI, and 0.2 U of the malate/lactate dehydrogenase of *Thermus thermophilus* HB8 (MLDH) (Ye et al., 2012), was used as a catalyst.

The reaction was performed at 70°C with stirring. Glucose (24 mM) and NAD^+ (10 mM) solution was supplied to the mixture at a flow rate of 1 μL min^{-1} (6 nmol glucose mL^{-1} min^{-1} and 2.5 nmol NAD^+ mL^{-1} min^{-1}, respectively) using a Shimadzu LC-20 AD solvent delivery unit. Aliquots (60 μl) of the reaction mixture were sampled at 1-h intervals and centrifuged to remove cell debris (15,000 rpm, 10 min). The supernatant was ultrafiltered using Amicon 3 K and then analyzed by HPLC.

3.2.8 Analytical methods

Fluorescence-labeled pyruvate was quantified by HPLC with a Cosmosil 5C18-ARII column (ϕ 4.6 × 150 mm, Nacalai Tesque, Kyoto, Japan). The column was eluted at 35°C using an eluent comprising 45% methanol and 1% acetic acid at a flow rate of 0.4 mL min^{-1}. The eluent was analyzed with a RF10A fluorescence detector (Shimadzu) at an excitation and emission wavelength of 360 and 415 nm, respectively. Lactate was analyzed by HPLC on two tandemly connected ion exclusion columns as described previously (Ye et al., 2012).

3.3 Results and Discussion

3.3.1 Gene assembly

Optimization of the metabolic balance is a crucial issue in achieving a high production rate via an artificially engineered pathway (Pfleger et al., 2006; Oliver et al., 2014; Nowroozi et al., 2014). Ye et al. (2012) demonstrated that the flux through an *in vitro* metabolic pathway can be spectrophotometrically determined by monitoring the concomitant consumption or production of NAD(P)H. This real-time monitoring technique enables us to identify rate-limiting enzymes in the *in vitro* pathway by increasing the concentration of each enzyme, one by one. The optimum ratio of enzyme concentrations to achieve a desired pathway flux can be experimentally determined by modulating the concentrations of the rate-limiting enzymes (Ye et al., 2012; Krutsakorn et al., 2013). A key challenge in constructing a multiple-gene-expression (MGE) recombinant strain producing a series of thermophilic enzymes is the reproduction of this optimized enzyme ratio *in vivo* by modulating the expression levels of the genes. Although the levels of gene expression are affected by many factors involving the promoter strength and translational efficiency, the author focused on the sequential order of the genes to limit the number of parameters. The use of a single operon prevents variation in transcriptional control (Pfleger et al., 2006), and the levels of cistrons transcribed within a single polycistronic mRNA tend to decrease with their distance from the promoter (Nishizaki et al., 2007). Based on this assumption, genes encoding the nine thermophilic enzymes involved in the chimeric glycolytic pathway were assembled into an artificial operon in an appropriate order.

To decide the gene order, the nine genes were individually introduced downstream of the Pr promoter of pRCI vector and expressed in *E. coli* DH5α. The mRNA

expression levels and the specific activities of the encoded enzymes in the resulting single-gene-expression (SGE) strains were determined, and the copy numbers of mRNA required to produce 1 unit of the enzymes were estimated (Table 3.2, line 4). The enzyme concentrations required to achieve a pyruvate production rate of 0.005 μmol min^{-1} mL^{-1} were experimentally determined using the cell-free extracts of the SGE strains following the method described previously (Ye et al., 2012), and the levels of mRNA required to produce the optimum concentrations of the enzymes were calculated (Table 3.2, line 6). The results indicated that the gene encoding GAPN would need to be most abundantly expressed among the nine genes. Accordingly, the GAPN-encoding gene was assigned to the first position in the operon and followed by the genes encoding FBA, GK, ENO, PGM, PFK, PK, TIM, and PGI in this order (Table 3.2, line 7). The genes were assembled in this order and introduced under the control of the Pr promoter of a pGETS118 vector using OGAB method (Tsuge et al., 2003). Gel electrophoresis of the *Eco*RI-digested fragments of the resulting plasmid (designated as pGETS-CGP) gave bands with the expected sizes, confirming that the genes had been assembled in the correct order (Fig. 3.1).

Table 3.2 Gene expression and specific enzyme activity in single-gene-expression strains

Enzyme	GAPN	FBA	GK	ENO	PGM	PFK	PK	TIM	PGI
mRNA expression level ($\times 10^9$ copies mg^{-1} wet cells)	39.8	135	60.2	216	46.0	42.1	4.11	139	148
Specific enzyme activity ($\times 10^{-3}$ U mg^{-1} wet cells)	0.52	7.10	4.01	26.1	14.2	20.1	31.1	2010	4600
mRNA per unit of enzyme [a] ($\times 10^{10}$ copies)	7650	1900	1500	828	324	210	13.2	6.92	3.22
Optimized enzyme concentration [b] ($\times 10^{-3}$ U/mL)	6.03	16.4	19.2	11.1	21.1	30.1	15.4	9.10	19.0
Required mRNA level [c] ($\times 10^8$ copies/mL)	4615	3118	2882	919	684	632	20.3	6.28	6.12
Gene order	1	2	3	4	5	6	7	8	9

[a] The copy numbers of mRNA required to produce 1 U each of the enzyme were calculated by dividing the mRNA expression level (line 2) by the specific enzyme activity (line 3).

[b] Enzyme concentrations were experimentally optimized to achieve a glucose consumption rate of 2.5 nmol min^{-1} mL^{-1}.

[c] The levels of mRNA required to produce the optimized concentration of the enzyme were calculated by multiplying mRNA per unit of enzyme (line 4) and the optimized enzyme concentrations (line 5).

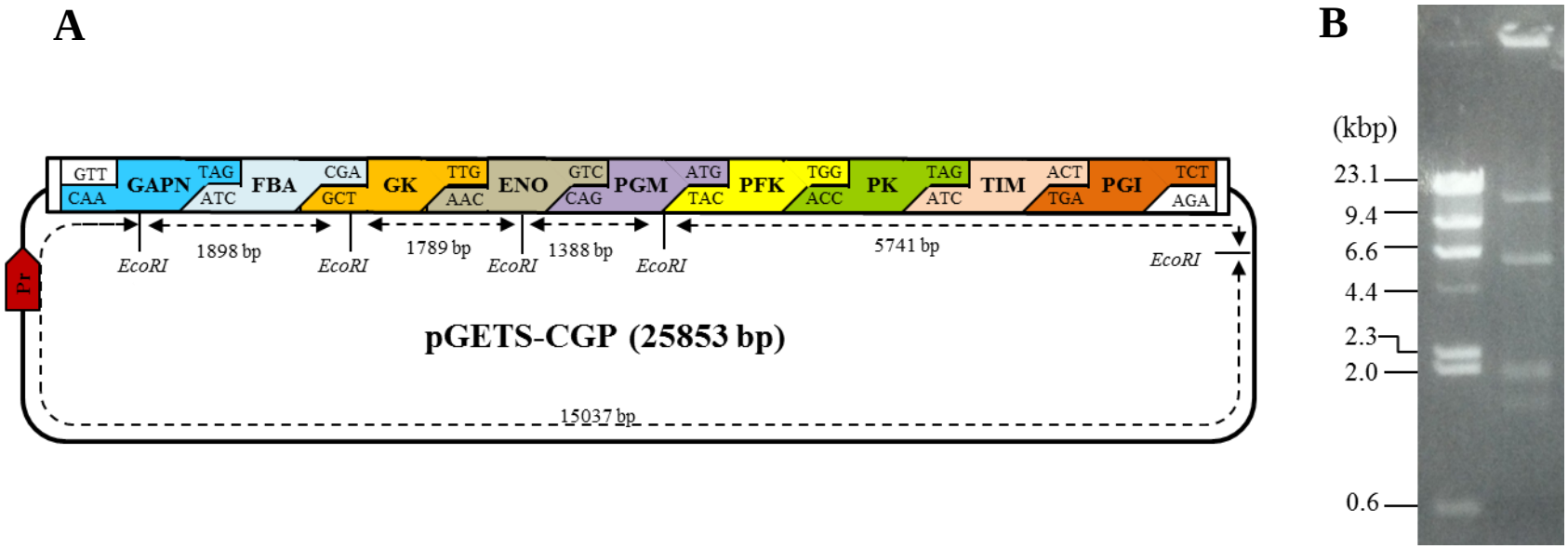

Fig. 3.1 (A) Schematic illustration of pGETS-CGP. *Eco*RI restriction sites and the estimated sizes of the *Eco*RI-digested fragments are shown. (B) Agarose gel electrophoresis of *Eco*RI-digested pGETS-CGP. Approximately 0.1 μg of pGETS-CGP was digested with *Eco*RI and separated by gel electrophoresis (right lane). *Hin*dIII-digested λ DNA was used as a size marker (left lane).

3.3.2 Expression profile of the assembled genes

The mRNA expression profile of the nine thermophilic glycolytic genes in the MGE strain was determined by RT-PCR (Fig. 3.2). The rank order of the gene expression levels corresponded to their sequential order in the constructed operon, except that the expression levels of the genes encoding ENO and PGM were unexpectedly high compared with those of other genes. This result may be explained by the possible presence of an intragenic promoter, which might be generated by the codon optimization, within the gene coding for GK. High mRNA levels of ENO- and PGM-encoding genes may also be due to the difference in the stabilities of the cistrons. Although the underlying reasons remain to be determined, differences in the stabilities of cistrons within a polycistronic mRNA have also been observed in naturally occurring operons in *E. coli* (Esquerré et al., 2014). Different levels of influence of *cis*-acting RNA elements and intrinsic endoribonucleases on the cistrons may account for differences in their stabilities.

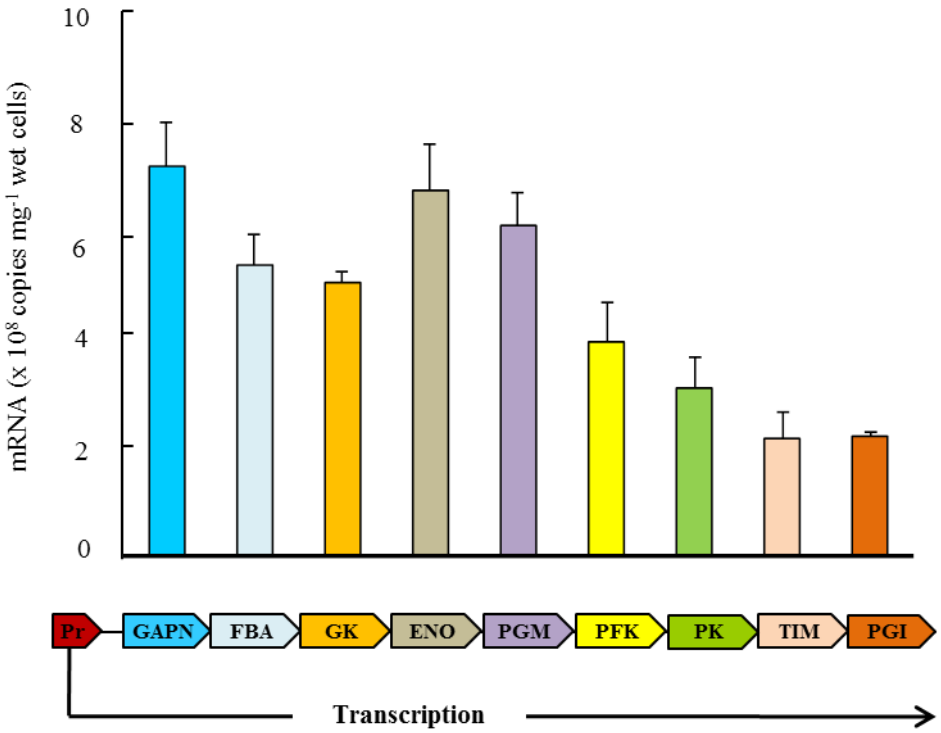

Fig. 3.2 mRNA expression levels of thermophilic glycolytic genes in multi-gene-expression *E. coli* cells. The RT-PCR data were obtained from at least three independent experiments and are shown as means ± standard deviations.

SDS-PAGE showed that most indigenous proteins in the cell-free extract of *E. coli* without pGETS-CGP were denatured by heat treatment at 70°C for 30 min (Fig. 3.3A, lane 2). In contrast, the heat-treated cell-free extract of the recombinant *E. coli* with pGETS-CGP showed extra protein bands that were not found in that of *E. coli* without the expression vector (Fig. 3.3A, lane 4). The heterologous production of the nine thermophilic enzymes in the recombinant *E. coli* were confirmed by visual comparison of the electrophoretic mobilities of these extra protein bands with those in the heat-treated cell-free extracts of the SGE strains (Fig. 3.3B). The mobility of the

recombinant PGM on the SDS-polyacrylamide gel was not consistent with its calculated molecular mass, probably owing to the aberrant migration of the protein. In addition, enzyme assays also showed that all of the nine genes were functionally expressed in the MGE strain (Table 3.3). The activities of the glycolytic enzymes in the heat-treated (70°C for 30 min) cell-free extract of *E. coli* with pGETS118 (empty vector) were below the detection level (data not shown). The specific enzyme activities in the cell-free extract of the MGE strain were compared with those in the enzyme cocktail prepared from a mixture of the SGE strains. The ratio of the cell concentrations in the mixture of the SGE strains were tuned to provide the optimized enzyme concentrations required for achieving a pyruvate production rate of 0.005 μmol min^{-1} mL^{-1} (*i.e.*, they were equal to those shown in Table 3.3, line 5). The specific activities in the MGE strain were 5.0 (FBA) to 1370 (PGM) times higher than those in the mixture of the SGE strains (Table 3.3).

Overproduction of a heterologous protein in recombinant microorganisms often results in improper folding of the protein and leads to the formation of an inclusion body. In fact, SDS-PAGE analysis of the soluble and insoluble fractions of the SGE strains revealed that a significant fraction of some enzymes (e.g., PFK and FBA) were accumulated as inclusion bodies. By contrast, others (e.g., ENO and GK) were mostly produced in the form of soluble active protein (Fig. 3.4). These observations indicated that the difference in the protein folding efficiency should also be taken into account to achieve more precise control of the expression levels of multiple genes. Overall, the accumulation of inclusion bodies appeared to be less significant in MGE strains, which partly accounts for higher specific activities in the MGE strain.

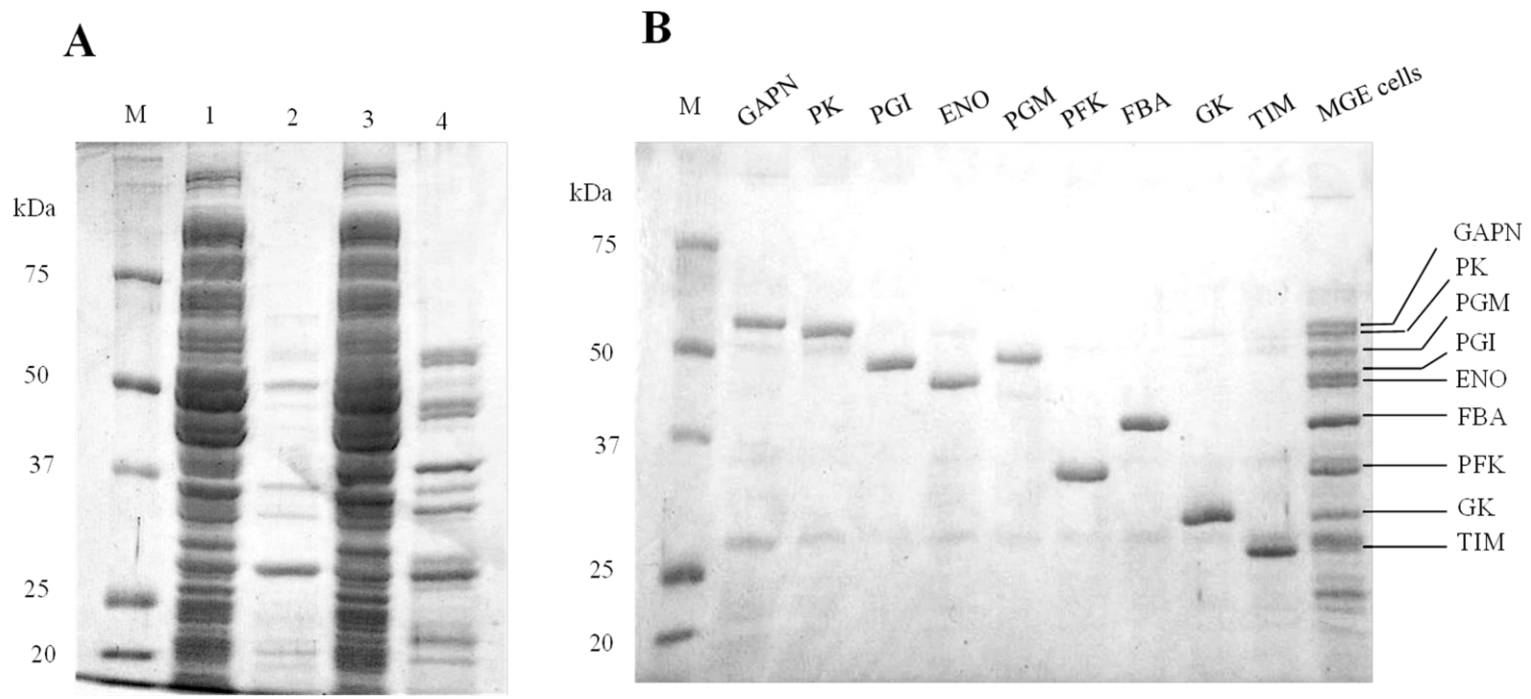

Fig. 3.3 (A) Protein expression in recombinant *E. coli* cells harboring pGETS118 (empty vector, lanes 1 and 2) and pGETS-CGP (lanes 3 and 4). Cell-free extracts were prepared using approximately 1 mg of wet cells and separated on 12% acrylamide gels before (lanes 1 and 3) and after (lanes 2 and 4) heat treatment at 70°C for 30 min. (B) SDS-PAGE of the heat-treated cell-free extracts of MGE and SGE cells. The calculated molecular mass of recombinant enzymes (kDa) are as follows: GAPN, 55.5; PK, 51.1; PGI, 46.1; ENO, 45.5; PGM, 45.1; PFK, 33.5; FBA, 40.3; GK, 31.5; and TIM, 27.0.

Table 3.3 Specific enzyme activities in multiple-gene-expression cells and a mixture of single-gene-expression cells [a].

Enzyme	GAPN	FBA	GK	ENO	PGM	PFK	PK	TIM	PGI
Multiple-gene-expression cells ($\times 10^{-3}$ U mg^{-1} wet cells)	1.81	1.69	4.10	158	577	44.8	371	23.1	10.3
Mixture of single-gene-expression cells [b] ($\times 10^{-3}$ U mg^{-1} wet cells)	0.12	0.32	0.38	0.22	0.42	0.60	0.30	0.18	0.38

[a] The enzyme assays were performed using the heat-treated cell-free extracts of the recombinant strains. The activities were normalized by the wet weight of the cells used for the preparation of the cell-free extracts (50 mg each for the multiple-gene-expression cells and the mixture of the single-gene-expression cells).

[b] Single-gene-expression cells producing GK, PGI, PFK, FBA, TIM, GAPN, PGM, ENO, and PK were mixed at the experimentally optimized ratio of 5: 1: 2: 5: 1: 32: 2: 1: 1 (wet weight).

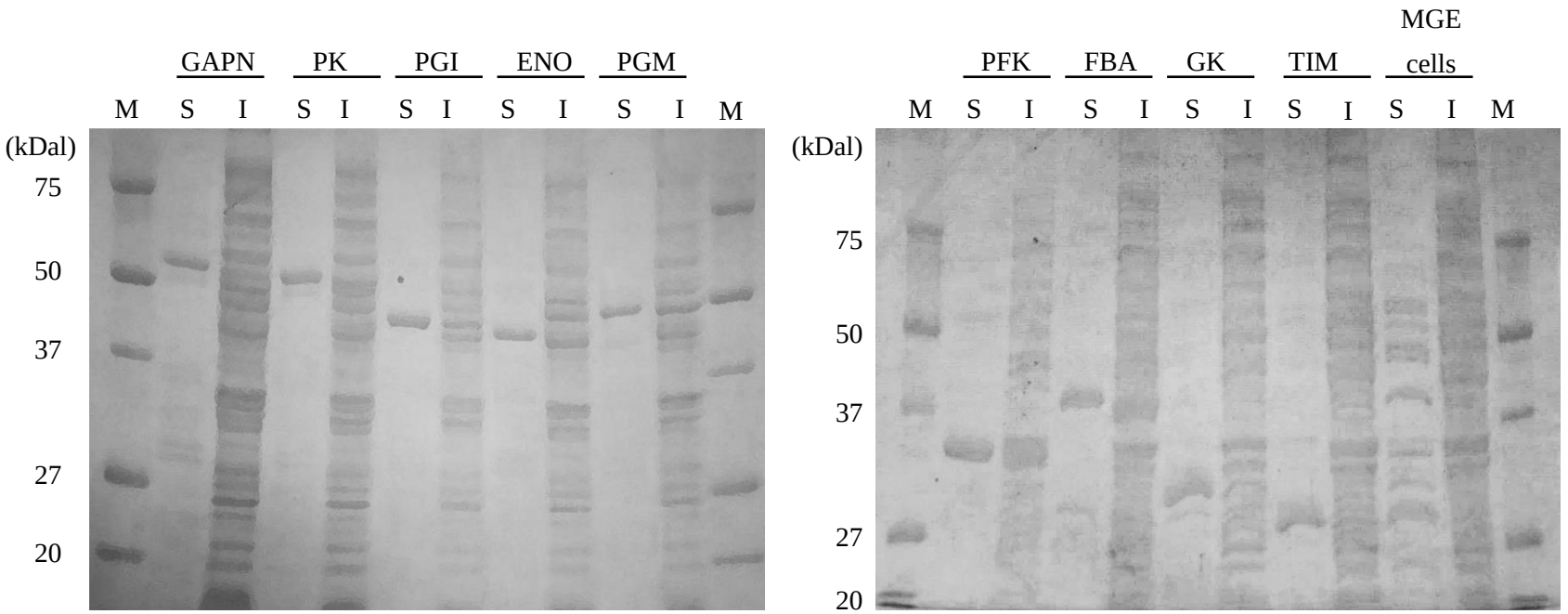

Fig. 3.4 SDS-PAGE analysis of the soluble (S) and insoluble (I) fractions of SGE and MGE cells. Crude extracts were prepared using approximately 1 mg of wet cells. Soluble and insoluble fractions were separated by centrifugation (15,000 × g, 15 min). Soluble fractions were heat-precipitated (70^{o}C, 30 min) and the resulting supernatants were analyzed. Insoluble fractions were washed once with the buffer and analyzed without the heat treatment.

3.3.3 Determination of the flux through the *in vitro* metabolic pathway

The pyruvate production rate through the cascade reaction with the nine thermophilic enzymes (*i.e.*, the flux through the chimeric glycolytic pathway) was determined using the MGE strain and the mixture of the SGE strains. The thermophilic NADH oxidase from *Thermococcus profundus*, which catalyzes the four-electron reduction of O_2 to H_2O using NADH as the electron donor (Jia et al., 2008), was added to the reaction mixture for cofactor regeneration. When 50 mg each of the wet cells of the MGE and the SGE strains were used, the MGE cells gave a 4.2-fold higher pyruvate production rate (Fig. 3.5). The high specific enzyme activities in the MGE cells (Table 3.3) likely contributed to this higher rate.

The use of heat-treated crude extracts of the MGE and SGE strains resulted in 1.4- and 2.1-fold higher pyruvate production rate, respectively than the direct use of the whole cells. This observation implied that the localization of the enzymes has a significant influence on the reaction rate. The membrane structure of *E. coli* cells is partially or entirely disrupted at high temperature and a fraction of the recombinant thermophilic enzymes, which are produced as soluble proteins, leaks out of the cells (Ninh et al., 2013; see also chapter 2). I quantified the levels of heat-induced leakage of enzymes from the MGE cells (Fig. 3.6). Although leakage levels varied among enzymes, more than 80% of the enzymes were retained in the cells even in the case of the most abundantly released enzyme (TIM). This fact indicated that the membrane structure of the recombinant *E. coli* was not entirely (but partly) disrupted under our experimental conditions. The barrier function of the cell membrane may impede substrate penetration into the cells to some extent, and result in the lower production rate observed in the whole-cell reactions. The lower production rate in the whole-cell bioconversion may

also be due to the highly crowded environment inside the cells. The total concentration of protein and RNA in an *E. coli* cell is in the range of 300-400 mg mL^{-1}, and they typically occupy 20-30% of the cytoplasmic volume of the cell (Ellis, 2001). As a result, diffusion of small molecules is three- to four-fold slower in the cell than that in pure water (Kao et al., 1993). Decrease in the diffusion rate of intermediates may result in lower flux though the artificial metabolic pathway inside the cells.

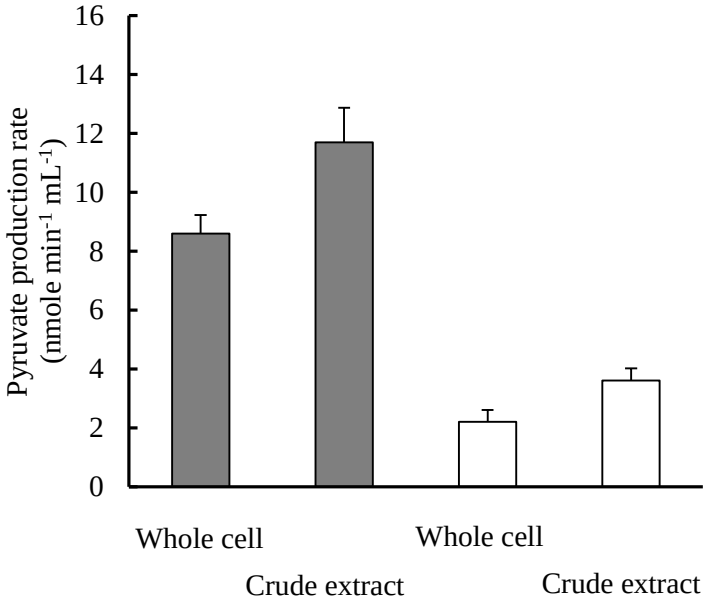

Fig. 3.5 Pyruvate production rate with the MGE strain (gray bars) and the mixture of nine SGE strains (white bars). Production rates were determined using either 50 mg (wet weight) of the whole cells or the crude extract prepared from equal weights of the wet cells. Single gene expression cells producing GK, PGI, PFK, FBA, TIM, GAPN, PGM, ENO, and PK were mixed at an experimentally optimized ratio of 5: 1: 2: 5: 1: 32: 2: 1: 1 (wet weight).

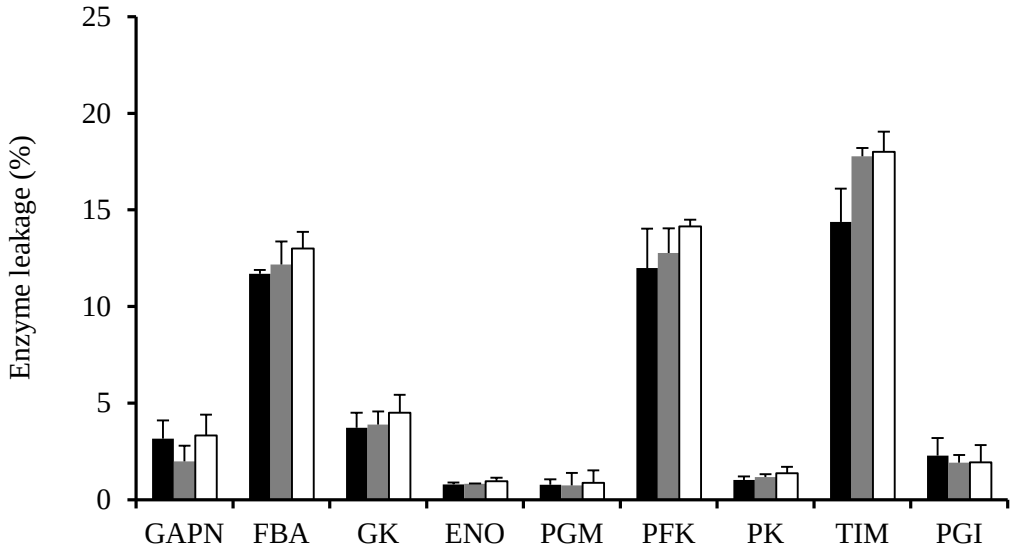

Fig. 3.6 Heat-induced leakage of enzymes from MGE cells. Cells were incubated at 70°C for 30 (black bars), 60 (gray bars), and 90 min (white bars). After removal of the cells by centrifugation, the levels of enzyme activities in the supernatant were determined under standard assay conditions. The leakage levels were expressed as the percentage of enzyme activity in cell-free extract prepared by ultrasonication.

3.3.4 Lactate production through the *in vitro* metabolic pathway

The heat-treated crude extract of the MGE cells was used as the catalyst for a one-pot conversion of glucose to lactate. MLDH, which catalyzes NAD^+-dependent reduction of pyruvate to lactate (Ye et al., 2012), was coupled with the *in vitro* glycolytic pathway for balancing the consumption and regeneration of the redox cofactor. An excess feeding of glucose to the *in vitro* pathway leads to rapid glucose phosphorylation by GK and results in an insufficient ATP pool size for further phosphorylation by PFK (Ye et al., 2012). Accordingly, the author supplied glucose in a fed-batch manner at the rate of 6 nmol min^{-1} mL^{-1}, which is one half of the experimentally determined pyruvate

production rate through the *in vitro* pathway (Fig. 3.5). NAD^+ was also continuously supplied to the reaction mixture at a rate identical to that of its thermal decomposition (2.5 nmol min^{-1} mL^{-1}) (Supplementary Fig. S2). The lactate production rate remained almost constant at the expected level (12 nmol min^{-1} mL^{-1}) for the initial 3 h (Fig. 3.7). Following this, 2.2 mM lactate was produced from 1.1 mM glucose with a molar yield of 100%, confirming that undesired side reactions could be eliminated by the thermal inactivation of indigenous enzymes. Decrease in the production rate became significant after the initial 3 h, and the molar yield of lactate production dropped to 82% at 4 h. This change appeared partly due to the dilution of the reaction mixture by the feeding of the substrate/cofactor solution (6.0% increase in the total volume at 4 h) and to the loss of enzymes by the sampling (4.5% decrease in the total concentration at 4 h). We also found that GK, PFK, ENO, and PK lost 20-25% of their activity after incubation at 70°C for 4 h (Fig. 3.8). Substitution of these enzymes with those derived from hyperthermophiles (*Sulfolobus solfataricus*, *Pyrococcus furiosus*, *Thermotoga maritima* or *Archaeoglobus profundus*) with higher optimum growth temperature than *T. thermophilus* may be a possible strategy for improving the operational stability of the *in vitro* metabolic pathway.

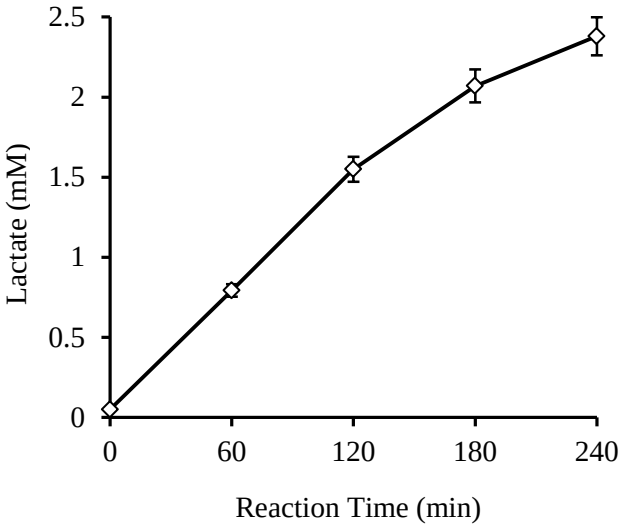

Fig. 3.7 Lactate production with a crude extract of MGE cells. The data shown as averages ± standard deviation (n = 3).

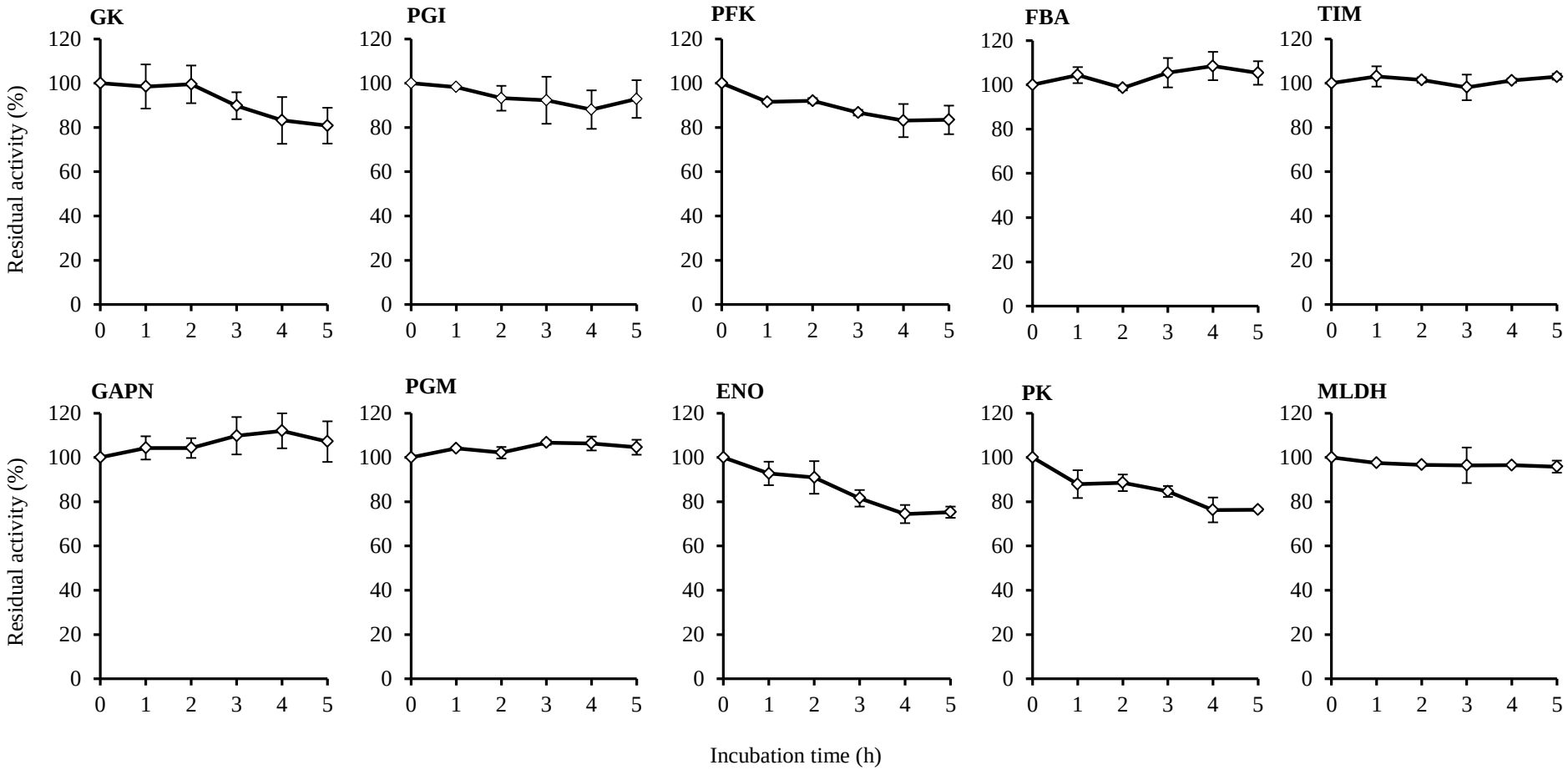

Fig. 3.8 Thermal stability of the enzymes. The single-gene-expression cells were disrupted and heat-treated at 70^{o}C for 30 min. After the removal of cell debris and denatured proteins by centrifugation, the enzyme solutions were incubated at 70^{o}C for indicated times. Residual enzyme activities were determined under the standard assay conditions.

3.4 Summary

In chapter 3, genes encoding nine thermophilic glycolytic enzymes were assembled in an artificial operon and co-expressed in a single recombinant *E. coli* strain. Gene expression levels of the recombinant thermophilic enzymes were controlled by their sequential order in the artificial operon. By simply heating a crude extract of the resulting recombinant cells, the *in vitro* synthetic pathway could be reconstituted without undesired side reaction and used for the one-pot production of pyruvate and lactate. In addition, it is noteworthy that the crude extract of the recombinant cells gave a markedly higher production rate than the whole-cell catalyst, probably owing to the barrier function of the cell membrane and/or the effects of macromolecular crowding. This observation poses a fundamental question about the validities of the mathematical models for simulating flux through an *in vivo* metabolic pathway with enzyme kinetic parameters obtained by *in vitro* experiments. This methodology, by which a highly simplified model pathway comprising only a limited number of active enzymes can be reconstituted inside cells, may contribute to the kinetic analysis of intracellular enzyme reactions and metabolisms.

4. Conclusions and future aspects

Implementation of a complex biochemical reaction through a cascade reaction with isolated enzymes offers some potential advantages over conventional fermentation-based processes. Since enzymatic reactions proceed independently on the biological activities of living organisms, reaction conditions can be more flexibly modified without a complex control of culture conditions. Theoretically, reaction rates are in proportion with enzyme concentration; therefore, reactions are more easily scaled up. Another important advantage of *in vitro* bioconversion is that the downstream processes can be greatly simplified as enzymatic reactions can be conducted in an inorganic buffer. Particularly, employment of thermophilic enzymes enables a one-step preparation of enzyme modules through a heat-treatment of recombinant mesophiles harboring heterologous thermotolerant enzymes and long-term operation of *in vitro* bioconversion system.

In this thesis, I aimed to further improve the operational simplicity of *in vitro* metabolic engineering approach with thermophilic enzymes. In chapter 2, a simple and unique approach for the preparation of the themophilic whole-cell biocatalyst was developed using glutaraldehyde and demonstrated to be applicable to repeated and continuous bioconversion system. With a simple pre-treatment of recombinant *E. coli*

cells having the thermophilic fumarase with 0.11% (vol/vol) of glutaraldehyde, a compromise between the heat-induced leakage and the remaining specific activity of the enzyme could be achieved. The heat-treatment of GA-treated *E. coli* cells resulted in a significant improvement in membrane permeability to relatively small molecules whereas the overall cellular structure was not apparently changed. The GA-treated cells having the thermophilic fumarase were then used as whole-cell biocatalysts for hydration of fumarate to malate in a continuous reactor at 70^{o}C. Consequently, 60% or higher conversion yield could be retained for at least more than 10h.

Chapter 3 demonstrated the assembly and co-expression of multiple genes encoding thermophilic enzymes in a single *E. coli* cell. Genes encoding nine enzymes involved in the chimeric Emben-Meyerhof pathway have been assembled in an artificial operon and functionally expressed in a single *E. coli* cell. By simply heating the crude extract of the recombinant *E. coli* strain, the *in vitro* pathway consisting of heterologously overproduced enzymes could be constructed. The resulting *in vitro* pathway could be used for the direct conversion of glucose to lactate with a molar yield of 82% by coupling with a thermophilic malate/lactate dehydrogenase.

One of the possible ideal goals of *in vitro* metabolic engineering would be the co-expression of the series of thermophilic enzymes in a single recombinant *E. coli*

followed by the GA-mediated membrane consolidation, and their application to a continuous bioconversion system. To demonstrate the applicability of the MGE cells in a repeated reaction, the cells were treated with 0.11% (vol/vol) GA and used for lactate bioconversion in the fed-batch system as described in chapter 3. The enzyme leakage from the MGE cells pre-treated with GA was kept under a detectable level after incubation at 70^{o}C for 60 min. In lactate bioconversion, the reaction was repeatedly performed with stirring at 70^{o}C. The GA-treated cells were recycled by centrifugation after being allowed to react for 2 h and subjected to a new reaction cycle. As a control experiment, the reaction using free cells was also carried out. Although the slight decrease in lactate yield was observed probably due to thermal inactivation of enzymes in GA-treated MGE cells, the product yield was remained above 0.30 mM after 7 repetitions (Fig. 4.1). By contrast, the lactate yield in reaction using free MGE cells was steeply decreased in repeated reactions. This result indicates that the GA-treated MGE cells could be used in repeated and continuous bioconversion systems.

As described in chapter 3, I found that the heat-treated crude extract showed a significantly higher production rate than the whole-cell catalysts, probably owing to the barrier function of the cell membrane and/or the effects of macromolecular crowding. Elucidation of the underlying mechanisms on the lower catalytic performance of the

whole-cell catalysts would be crucial issue for achieving both the reusability and the sufficient conversion rate. In chapter 2, I focused predominantly on the effects of GA concentration on the leakage levels and activity of enzyme. However, more detailed investigations on other parameters, including the time and temperature for heat-treatment, may lead to the improvement of the membrane permeability and the higher reaction rate can be achieved.

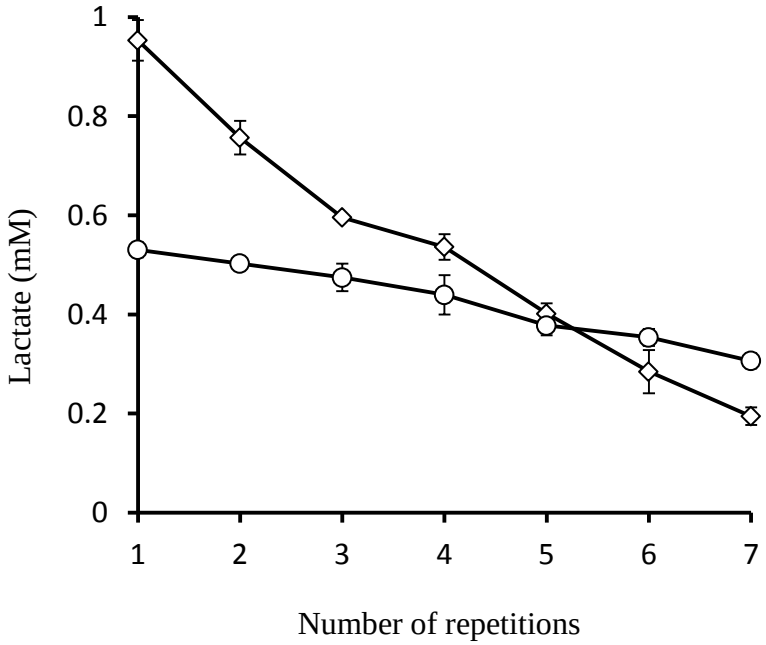

Fig. 4.1 Reusabilities of free (diamonds) and GA-treated MGE (circles) cells. Each reaction was performed at 70^{o}C for 2 h. The data are shown as averages ± standard deviations (n = 3).

A combination of GA-treated cells with a cell-separation filter is a simple and efficient method to operate a continuous reaction. However, this system is difficult to be applied to the separation between the desired product and other small molecules. Particularly, eluent of cofactors from the reactor prevents their continuous use during the long-term reaction. Several methods have been developed for the retention of cofactors in continuous reactors. One of these methods is immobilization of cofactors (e.g., $NAD(P)^+$/NAD(P)H) on water-soluble polymers such as polyethylene glycol (Wichmann and Wandrey, 1981; Hummel et al., 1988), dextran (Gu and Chang, 1990) and polyethyleneimine (Obón et al., 1998). The immobilization of cofactors to polymers with molecular weights of 2-3 kDa, which can diffuse into the GA- and heat-treated cells (see chapter 2), can be retained in the continuous reactor using an ultrafiltration membrane and separated from product solution.

References

Adrio JL, Demain AL. 2014. Microbial enzymes: Tools for biotechnological processes. Biomolecules 4:117-139.

Ajikumar PK, Xiao WH, Tyo KEJ, Wang Y, Simeon F, Leonard E, Mucha O, Phon TH, Pfeifer B, Stephanopoulos G. 2010. Isoprenoid pathway optimization for taxol precursor overproduction in *Escherichia coli*. Science 330:70-74.

Ajinomoto, 2013. FY2013 market and other information. http://www.ajinomoto.com/en/ir/pdf/FY13_Data_E.pdf.

Arroyo M, de la Mata I, Acebal C, Castillón MP. 2003. Biotechnological applications of penicillin acylases: state-of-the-art. Appl Microbiol Biotechnol 60:507-514.

Atsumi S, Hanai T, Liao JC. 2008. Non-fermentative pathways for synthesis of branched-chain higher alcohols as biofuels. Nature 415:86-89.

Bae HS, Lee SG, Hong SP, Kwak MS, Esaki N, Soda K, Sung MH. 1999. Production of aromatic D-amino acids from α-keto acids and ammonia by coupling of four enzyme reactions. J Mol Cat B: Enzym 6:241-247.

Bhattacharya S, Schiavone M, Gomes J, Bhattacharya SK. 2004. Cascade of bioreactors in series for conversion of 3-phospho-D-glycerate into D-ribulose-1,5-bisphosphate: kinetic parameters of enzymes and operation variables. J Biotechnol 111:203-217.

BBC research, 2014. Global markets for enzymes in industrial applications. A BBC research biotechnology report (BI0034).

Bommarius AS, Schwarm M, Stingl M, Kotterhahn K, Huthmacher K, Drauz K. 1995. Synthesis and use of enantiomerically pure *tert*-leucine. Tetrahedron: Asymmetry 6 (12): 2851-2888.

Bornscheuer UT, Huisman GW, Kazlauskas RJ, Lutz S, Moore JC, Robins K. 2012. Engineering the third wave of biocatalysis. Nature 485:185-194.

Burda E, Hummel W, Gröger H. 2008. Modular chemoenzymatic one-pot syntheses in aqueous media: Combination of a palladium-catalyzed cross-coupling with an asymmetric biotransformation. Angew Chem Int 47:9551-9554.

Cava F, Hidalgo A, Berenguer J. 2009. *Thermus thermophilus* as biological model. Extremophiles 13:213-231.

Chen RR. 2007. Permeability issues in whole-cell bioprocesses and cellular membrane engineering. Appl Microbiol Biotechnol 74:730-738.

Choi YJ, Lee SY. 2013. Microbial production of short-chain alkanes. Nature 502:571-574.

De Regil R, Sandoval G. 2013. Biocatalysis for biobased chemicals. Biomolecules 3(4):812-847.

Decad GM, Nikaido H. 1976. Outer membrane of gram-negative bacteria XII. Molecular-sieving function of cell wall. J Bacteriol 128:325-336.

DiCosimo R, McAuliffe J, Poulose AJ, Bohlmann G. 2013. Industrial use of immobilized enzymes. Chem Soc Rev 42:6437.

Ellis RJ. 2001. Macromolecular crowding: obvious but underappreciated. Trends Biochem Sci 26:597-604.

Elander RP. 2003. Industrial production of β-lactam antibiotics. Appl Microbiol Biotechnol 61:385-392.

Esquerré T, Laguerre S, Turlan C, Carpousis AJ, Girbal L, Cocaign-Bousquet M. 2014. Dual role of transcription and transcript stability in the regulation of gene expression in *Escherichia coli* cells cultured on glucose at different growth rates. Nucleic Acids

Res 42 (4):2460-2472.

Fernández-Lorente G, Palomo JM, Mateo C, Munilla R, Ortiz C, Cabrera Z, Guisán JM, Lafuente RF. 2006. Glutaraldehyde cross-linking of lipases adsorbed on aminated supports in the presence of detergents leads to improved performance. Biomacromolecules 7:2610-2615.

Gänzle MG. 2012. Enzymatic synthesis of galacto-oligosaccharides and other lactose derivatives (hetero-oligosaccharides) from lactose. Int Dairy J 20:116-122.

Giuliano M, Schiraldi C, Marotta MR, Hugenholtz J, De Rosa M. 2004. Expression of *Sulfolobus solfataricus* α-glucosidase in *Lactococcus lactis*. Appl Microbiol Biotechnol 64:829-832.

Gröger H, Asano Y. 2012. Principles and historical landmarks of enzyme catalysis in organic synthesis. Enzyme catalysis in organic synthesis, third edition. Edited by Karlheinz Drauz, Harald Gröger, and Oliver May, Wiley-VCH. p1-42.

Gu KF, Chang TMS. 1990. Production of essential L-branched-chain amino acids in bioreactors containing artificial cells immobilized multienzyme system and dextran-NAD^+. Biotechnol Bioeng 36:263-269.

Gupta R, Beg QK, Lorenz B. 2002. Bacterial alkaline proteases: molecular approach and industrial application. Appl Microbiol Biotechnol 59:15-32.

Guterl J-K, Garbe D, Carsten J, Steffler F, Sommer B, Reiße S, Philipp A, Haack M, Rühmann B, Koltermann A, Kettling U, Brück T, Sieber V. 2012. Cell-free metabolic engineering: Production of chemicals by minimized reaction cascades. Chem Sus Chem 5(11):2165-2172.

Habeeb AFSA, Hiramoto R. 1968. Reaction of proteins with glutaraldehyde. Arch Biochem Biophys 126:16-26.

Hiroe A, Tsuge K, Nomura CT, Itaya M, Tsuge T. 2012. Rearrangement of gene order in the *pha*CAB operon leads to effective production of ultrahigh-molecular-weight poly[(R)-3-hydrobutyrate] in genetically engineered *Escherichia coli*. Appl Environ Microbiol 78:3177-3184.

Honda K, Maya S, Omasa T, Hirota R, Kuroda A, Ohtake H. 2010. Production of 2-deoxyribose 5-phosphate from fructose to demonstrate a potential of artificial bio-synthetic pathway using thermophilic enzymes. J Biotechnol 148:204-207.

Hummel W, Schiitte H, Kula MR. 1988. D-(-)-Mandelic acid dehydrogenase from *Lactobacillus curvatus*. Appl Microbiol Biotechnol 28:433-439.

Jia B, Park SC, Lee S, Pham BP, Yu R, Han SW, Yang JK, Choi MS, Baumeister W, Cheong GW. 2008. Hexameric ring structure of a thermophilic archaeon NADH oxidase that produces predominantly H_2O. FEBS J 275:5355-5366.

Johannes, TW, Zhao H. 2006. Directed evolution of enzymes and biosynthetic pathways. Curr Opin Microbiol 9:261-267.

Kaneko S, Akioka M, Tsuge K, Itaya M. 2005. DNA shuttling between plasmid vectors and a genome vector: systematic conversion and preservation of DNA libraries using the *Bacillus subtilis* genome (BGM) vector. J Mol Biol 349:1036-1044.

Kao HP, Abney JR, Verkman AS. 1993. Determinants of the translational mobility of a small solute in cell cytoplasm. J Cell Biol 120:175-184.

Kieliszek M, Misiewicz A. 2014. Microbial transglutaminase and its application in the food industry. Folia Microbiol 59:241-250.

Kikuchi H, Inoue M, Saito H, Sakurai H, Aritsuka T, Tomita F, Yokota A. 2009. Industrial production of difructose anhydride III (DFA III) from crude inulin extracted from chicory roots using Arthrobactersp. H65-7 fructosyltransferase. J

Biosci Bioeng 107(3):262-265.

Kim BW, Kim HW, Nam SW. 1997. Continuous production of fructose-syrups from inulin by immobilized inulinase from recombinant *Saccharomyces cerevisiae*. Biotechnol Bioprocess Eng 2:90-93.

Krutsakorn B, Honda K, Ye X, Imagawa T, Bei X, Okano K, Ohtake H. 2013. *In vitro* production of *n*-butanol from glucose. Metab Eng 20:84-91.

Lods LM, Dres C, Johnson C, Scholz DB, Brooks GJ. 2000. The future of enzymes in cosmetics. Inter J Cosm Sci 22:85-94.

McGucken PV, Woodside W. 1973. Studies on the mode of action of glutaraldehyde on *Escherichia coli*. J Appl Bact 36:419-426.

Migneault I, Dartiguenave C, Bertrand MJ, Waldron KC. 2004. Glutaraldehyde: behavior in aqueous solution, reaction with proteins, and application to enzyme crosslinking. BioTechniques 37:790-802.

Minamida K, Asakawa C, Sujaya N, Kaneko M, Abe A, Sone T, Hara H, Asano K, Tomita F. 2006. Effects of long-term ingestion of difructose anhydride III (DFA III) on intestinal bacteria and bile acid metabolism in humans. J Biosci Bioeng 101(2):149-156.

Munton TJ, Russell AD. 1970. Aspects of the action of glutaraldehyde on *Escherichia coli*. J Appl Bact 33:410-419.

Mühling J, Fuchs M, Campos ME, Gonter J, Engel JM, Sablotzki A, Menges T, Weiss S, Dehne MG, Krüll M, Hempelmann G. 2003. Quantitative determination of free intracellular α-keto acids in neutrophils. J Chromatogr B 789:383-392.

Muñoz Solano D. Hoyos P, Hernáiz MJ, Alcántara AR, Sánchez-Montero JM. 2012. Industrial biotransformations in the synthesis of building blocks leading to

enantiopure drugs. Bioresour Technol 115:196-207.

Myung S, Rollin J, You C, Sun F, Chandayan S, Adams MWW, Zhang YHP. 2014. *In vitro* metabolic engineering of hydrogen production at theoretical yield from fructose. Metab Eng 24:70-77.

Nakamura CE, Whited GM. 2003. Metabolic engineering for the microbial production of 1,3-propanediol. Curr Opin Biotechnol 14: 454-459.

Nimni ME, Cheung D, Strates B, Kodama M, Sheikh K. 1987. Chemically modified collagen: a natural biomaterial for tissue replacement. J Biomed Mater Res 21:741-771.

Ninh PH, Honda K, Yokohigashi Y, Okano K, Omasa T, Ohtake H. 2013. Development of a continuous bioconversion system using a thermophilic whole-cell biocatalyst. Appl Environ Microbiol 79:1996-2001.

Nishizaki T, Tsuge K, Itaya M, Doi N, Yanagawa H. 2007. Metabolic engineering of carotenoid biosynthesis in *Escherichia coli* by ordered gene assembly in *Bacillus subtilis*. Appl Environ Microbiol 73:1355-1361.

Nowroozi FF, Baidoo EEK, Ermakov S, Redding-Johanson, AM, Batth T, Petzold CJ, Keasling JD. 2014. Metabolic pathway optimization using ribosome binding site variants and combinatorial gene assembly. Appl Microbiol Biotechnol 98:1567-1581.

Obón JM, Manjón A, Iborra JL. 1998. Retention and regeneration of native NAD(H) in non-charged ultrafiltration membrane reactors: application to L-lactate and gluconate production. Biotechnol Bioeng 57:510-517.

Okuda K, Urabe I, Yamada Y, Okada H. 1991. Reaction of glutaraldehyde with amino and thiol compounds. J Ferment Bioeng 71:100-105.

Oliver JWK, Machado IMP, Yoneda H, Atsumi S. 2014. Combinatorial optimization of cyanobacterial 2,3-butanediol production. Metab Eng 22:76-82.

Opgenorth PH, Korman TP, Bowie JU. 2014. A synthetic biochemistry molecular purge valve module that maintains redox balance. Nature Commun 5:4113.

Osborn HT, Akoh CC. 2002. Structured lipids-novel fats with medical, nutraceutical, and food applications. Compr Rev Food Sci Food Saf 3:110-120.

Paddon CJ, Westfall PJ, Pitera DJ, Benjamin K, Fisher K, McPhee D, Leavell MD, Tai A, Main A, Eng D, Polichuk DR, Teoh KH, Reed DW, Treynor T, Lenihan J, Fleck M, Bajad S, Dang G, Diola D, Dorin G, Ellens KW, Fickes S, Galazzo J, Gaucher SP, Geistlinger T, Henry T, Hepp M, Horning T, Iqbal T, Jiang H, Kizer L, Lieu B, Melis D, Moss N, Regentin R, Secrest S, Tsuruta H, Vazquez R, Westblade LF, Xu L, Yu M, Zhang Y, Zhao L, Lievense J, Covello PS, Keasling JD, Reiling KK, Renninger NS, Newman JD. 2013. High-level semi-synthetic production of the potent antimalarial artemisinin. Nature 496:528-532.

Panesar PS, Kumari S, Panesar R. 2010. Potential applications of immobilized β-galactosidase in food processing industries. Enzym research 2010:473137.

Patel RN. 2013. Biocatalytic synthesis of chiral alcohols and amino acids for development of pharmaceuticals. Biomolecules 3:741-777.

Persidis A. 1998. Extremophiles. Nat Biotechnol 16:593-594.

Pfleger BF, Pitera DJ, Smolke CD, Keasling JD. 2006. Combinatorial engineering of intergenic regions in operons tunes expression of multiple genes. Nat Biotechnol 24:1027-1032.

Playne MJ, Crittenden RG. 2009. Galacto-oligosaccharides and other products derived from lactose. In: McSweeney PLH, Fox PF, editors. Lactose, water, salts and minor

constituents. 3rd ed. New York: Springer.p 121–201.

Presečki AV, Zelić B, Vasić-Rački Đ. 2007. Comparison of the L-malic acid production by isolated fumarase and fumarase in permeabilized baker's yeast cells. Enzym Microb Technol 41:605.

Presečki AV, Zelić B, Vasić-Rački Đ. 2009. Modeling of continuous L-malic acid production by porcine heart fumarase and fumarase in yeast cells. Chem Biochem Eng 23:519-525.

Rao MB, Tanksale AM, Ghatge MS, Deshpande VV. 1998. Molecular and biotechnological aspects of microbial proteases. Microbiol Mol Biol Rev 62:597-635.

Ren X, Yu D, Yu L, Gao G, Han S, Feng Y. 2007. A new study of cell disruption to release recombinant thermostable enzyme from *Escherichia coli* by thermolysis. J Biotechnol 129:668-673.

Restiawaty E, Iwasa Y, Maya S, Honda K, Omasa T, Hirota R, Kuroda A, Ohtake H. 2011. Feasibility of thermophilic adenosine triphosphate-regeneration system using using *Thermus thermophilus* polyphosphate kinase. Process Biochem 46:1747-1752.

Restiawaty E, Honda K, Okano K, Hirota R, Omasa T, Kuroda A, Ohtake H. 2012. Construction of membrane-anchoring fusion protein of *Thermococcus kodakarensis* glycerol kinase and its application to repetitive batchwise reactions. J Biosci Bioeng 113:521-525.

Rollin JA, Tam TK, Zhang YHP. 2013. New biotechnology paradigm: cell-free biosystems for biomanufacturing. Green Chem 15:1708-1719.

Römisch W, Eisenreich W, Richter G, Bacher A. 2002. Rapid one-pot synthesis of riboflavin isotopomers. Org Chem 67:8890-8894.

Sawai H, Mimitsuka T, Minegishi S, Henmi M, Yamada K, Shimizu S, Yonehara T. 2011. A novel membrane-integrated fermentation reactor system: application to pyruvic acid production in continuous culture by *Torulopsis glabrata*. Bioproc Biosyst Eng 34:721-725.

Schmid A, Dordick JS, Hauer B, Kiener A, Wubbolts M, Witholt B. 2001. Industrial biocatalysis today and tomorrow. Nature 409:258-268.

Shigematsu N, Okuhara Y, Shiomi T, Tomita F, Hara H. 2004. Effect of difructose anhydride III on calcium absorption in humans. Biosci Biotechnol Biochem 68:1011-1016.

Singh SR, Dhaliwal R, Puri M. 2008. Development of a stable continuous flow immobilized enzyme reactor for the hydrolysis of inulin. J Ind Microbiol Biotechnol 35:777-782.

Stojkovič G, Plazl I, Žnidaršič-Plazl P. 2011. L-Malic acid production within a microreactor with surface immobilised fumarase. Microfluid Nanofluid 10:627-635.

Tsuchido T, Katsui N, Takeuchi A, Takano M, Shibasaki I. 1985. Destruction of the outer membrane permeability barrier of *Escherichia coli* by heat treatment. Appl Environ Microbiol 50:298-303.

Tsuge K, Matsui K, Itaya M. 2003. One step assembly of multiple DNA fragments with a designed and orientation in *Bacillus subtilis* plasmid. Nucleic Acids Res 31(21):E113.

Turner P, Mamo G, Karlsson EN. 2007. Potential and utilization of thermophiles and thermostable enzymes in biorefining. Microb Cell Fact 6:9.

Vandamme E, Bienfait CG, 2004. Industrial biotechnology and sustainable chemistry. Royal Belgian Academy Council of Applied Science, p. 32.

Welch P, Scopes RK. 1985. Studies on cell-free metabolism: Ethanol production by a yeast glycolytic system reconstituted from purified enzymes. J Biotechnol 2:257-273.

Whited, GM, Feher FJ, Benko DA, Cervin MA, Chotani GK, McAuliffe JC, LaDuca RJ, Ben-Shoshan EA, Sanford KJ. 2010. Technology update: Development of a gas-phase bioprocess for isoprene-monomer production using metabolic pathway engineering. Ind Biotechnol 6:152-163.

Wichmann R, Wandrey C. 1981. Continuous enzymatic biotransformation in an enzyme membrane reactor with simultaneous NAD(H) regeneration. Biotechnol Bioeng 12:2789-2802.

Woeltinger J, Karau A, Leuchtenberger W, Drauz K. 2005. Membrane reactors at Degussa. Adv Biochem Engin/Biotechnol 92: 289-316.

Woodward J, Orr M, Cordaray K, Greenbaum E. 2000. Enzymatic production of biohydrogen. Nature 405:1014-1015.

Ye X, Honda K, Sakai T, Okano K, Omasa T, Hirota R, Kuroda A, Ohtake H. 2012. Synthetic metabolic engineering-a novel, simple technology for designing a chimeric metabolic pathway. Microb Cell Fact 11:120.

Ye X, Honda K, Morimoto Y, Okano K, Ohtake H. 2013. Direct conversion of glucose to malate by synthetic metabolic engineering. J Biotechnol 164(1):34-40.

Yokoyama S, Hirota H, Kigawa T, Yabuki T, Shirouzu M, Terada T, Ito Y, Matsuo Y, Kuroda Y, Nishimura Y, Kyogoku Y, Miki K, Masui R, Kuramitsu S. 2000. Structural genomics projects in Japan. Nat Struct Biol 7:943-945.

You C, Chen H, Myung S, Sathitsuksanoh N, Ma H, Zhang XZ, Li J, Zhang YHP. 2013. Enzymatic transformation of nonfood biomass to starch. Proc Natl Acad Sci USA

110:7182-7187.

Zhang B, Weng Y, Xu H, Mao Z. 2012. Enzyme immobilization for biodiesel production. Appl Microbiol Biotechnol 93:61-70.

Zhang Y-HP, Evans BR, Mielenz JR, Hopkins RC, Adams MWW. 2007. High-yield hydrogen production from starch and water by a synthetic enzymatic pathway. PLoS ONE 2(5):e456.

Zhang Y-HP, Myung S, You C, Zhu Z, A. Rollin J. 2011. Toward low-cost biomanufacturing through *in vitro* synthetic biology: bottom-up design. J Mater Chem 21:18877-18886.

Zheng GW, Xu JH. 2011. New opportunities for biocatalysis: driving the synthesis of chiral chemicals. Curr Opin Biotechnol 22:784-792.

Zhu F, Zhong X, Hu M, Lu L, Deng Z, Liu T. 2014. *In vitro* reconstitution of mevalonate pathway and targeted engineering of farnesene overproduction in *Escherichia coli*. Biotechnol Bioeng 111(7):1396-1404.

Zhu Z, Tam TK, Sun F, You C, Zhang YHP. 2014. A high-energy-density sugar biobattery based on a synthetic enzymatic pathway. Nat Commun 5:3026.

Supplementary figure S1

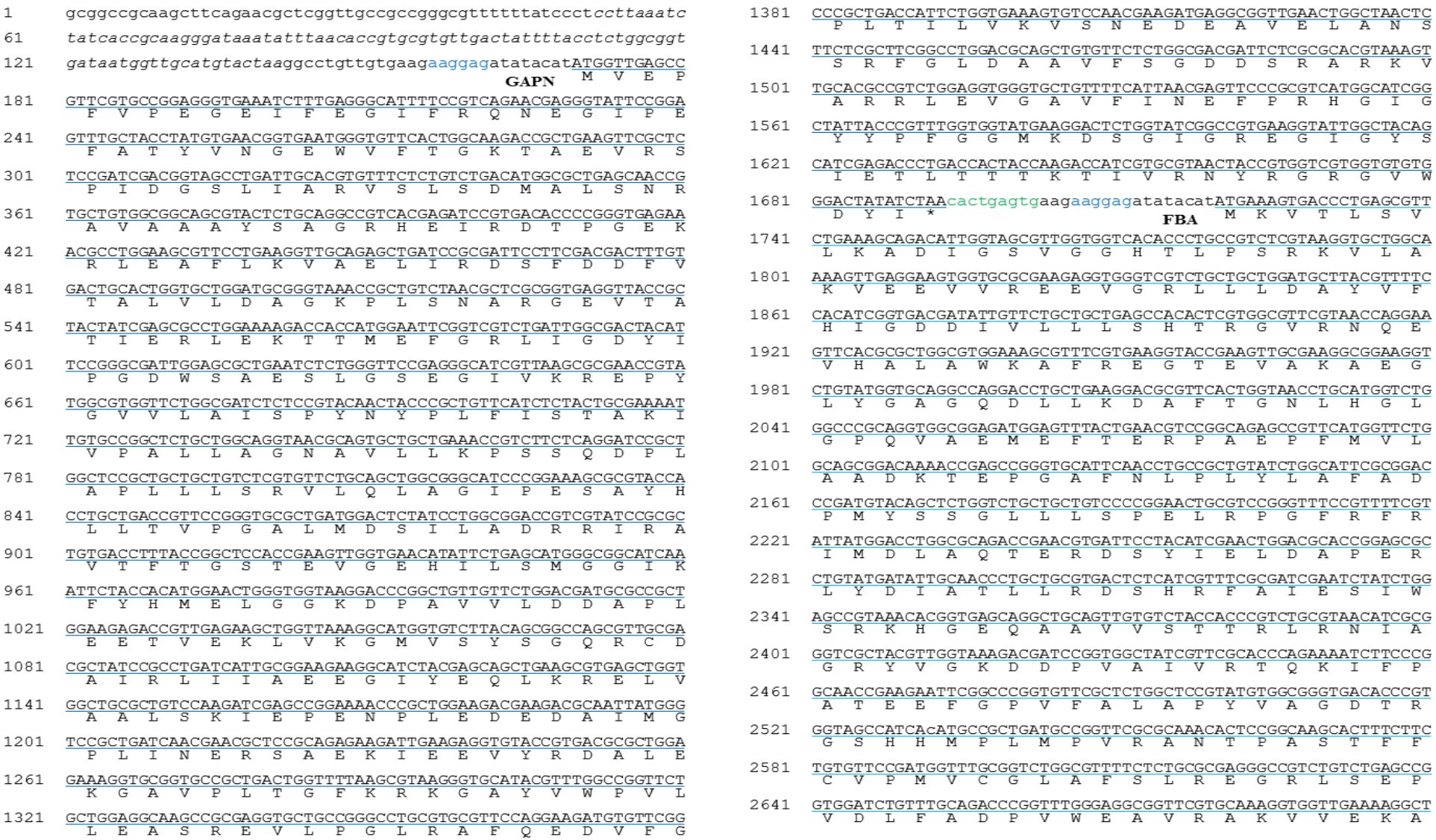

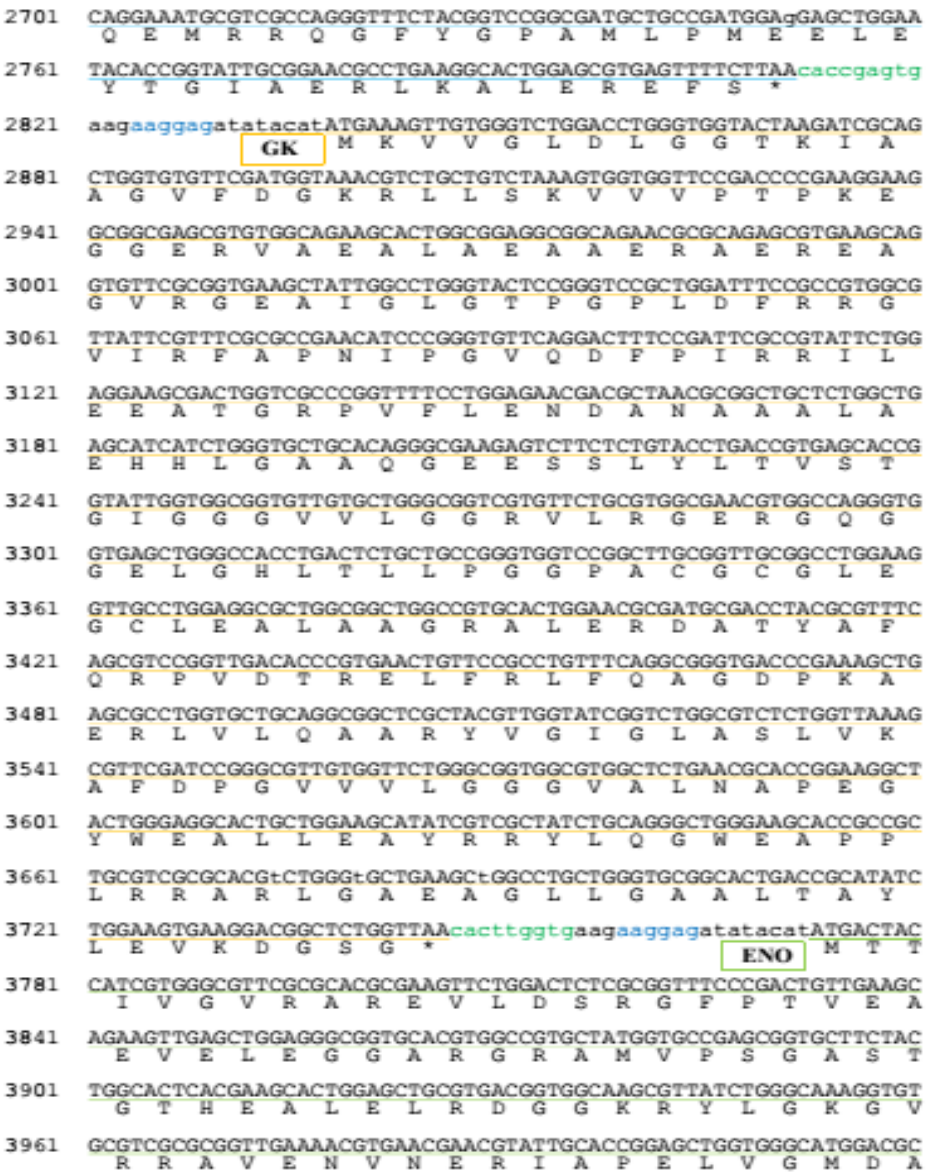
GK
ENO

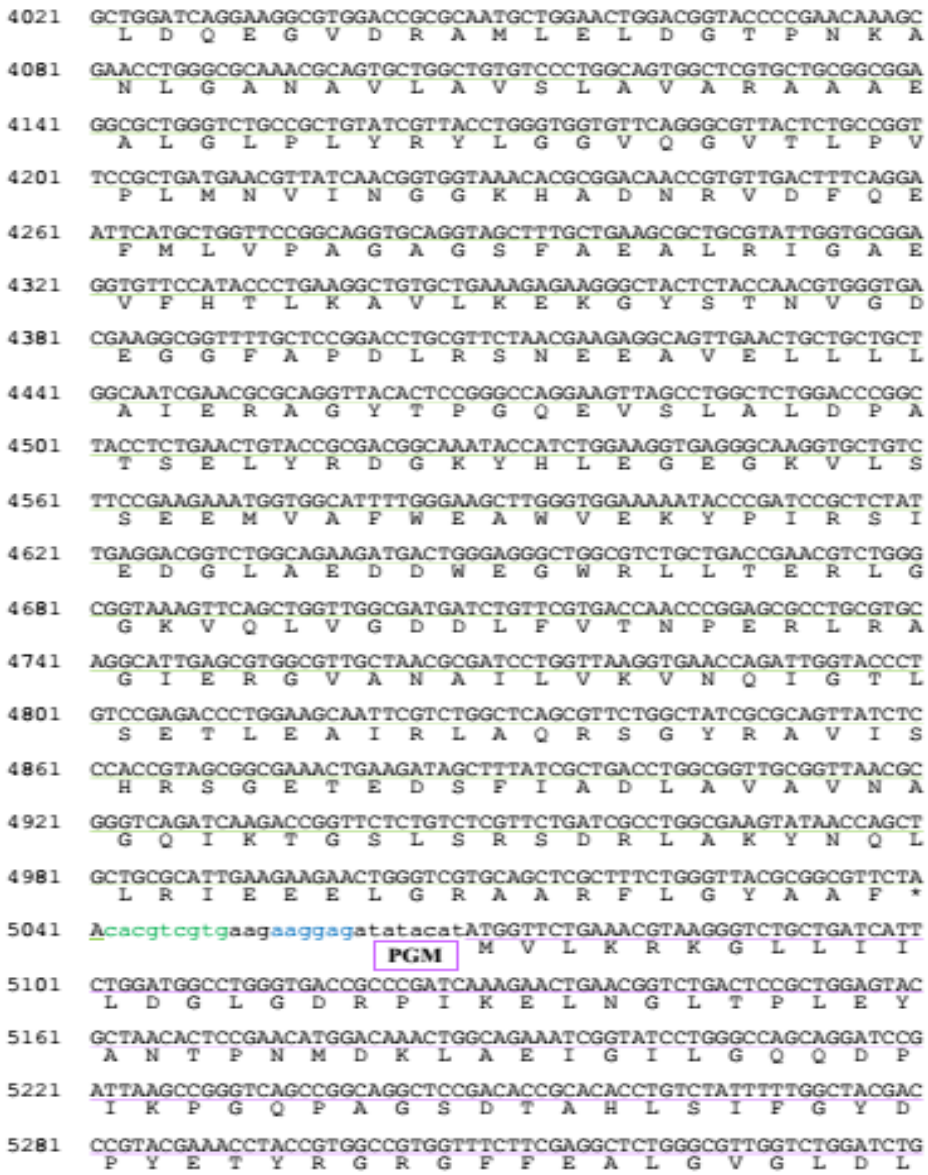
PGM

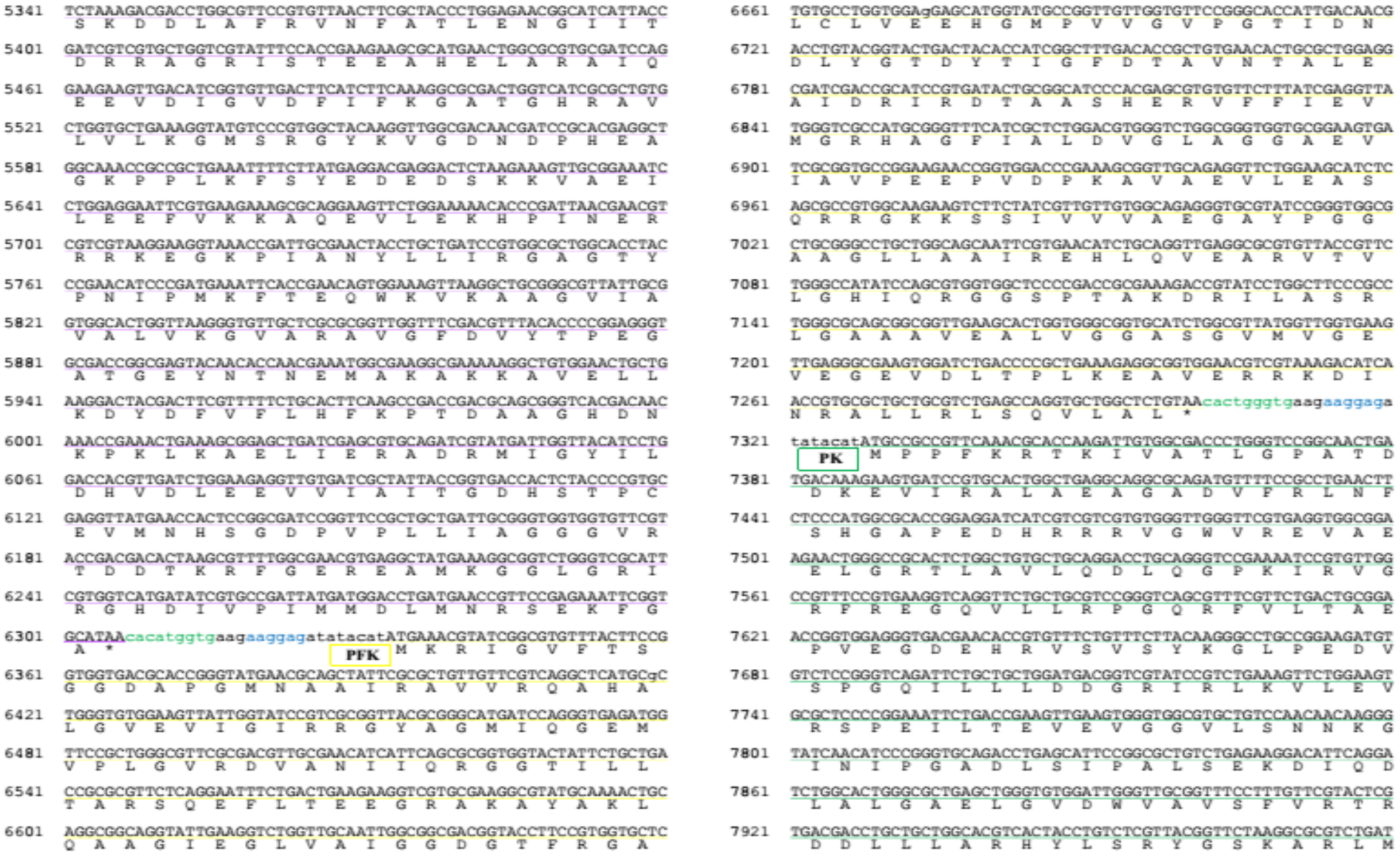
PFK
PK

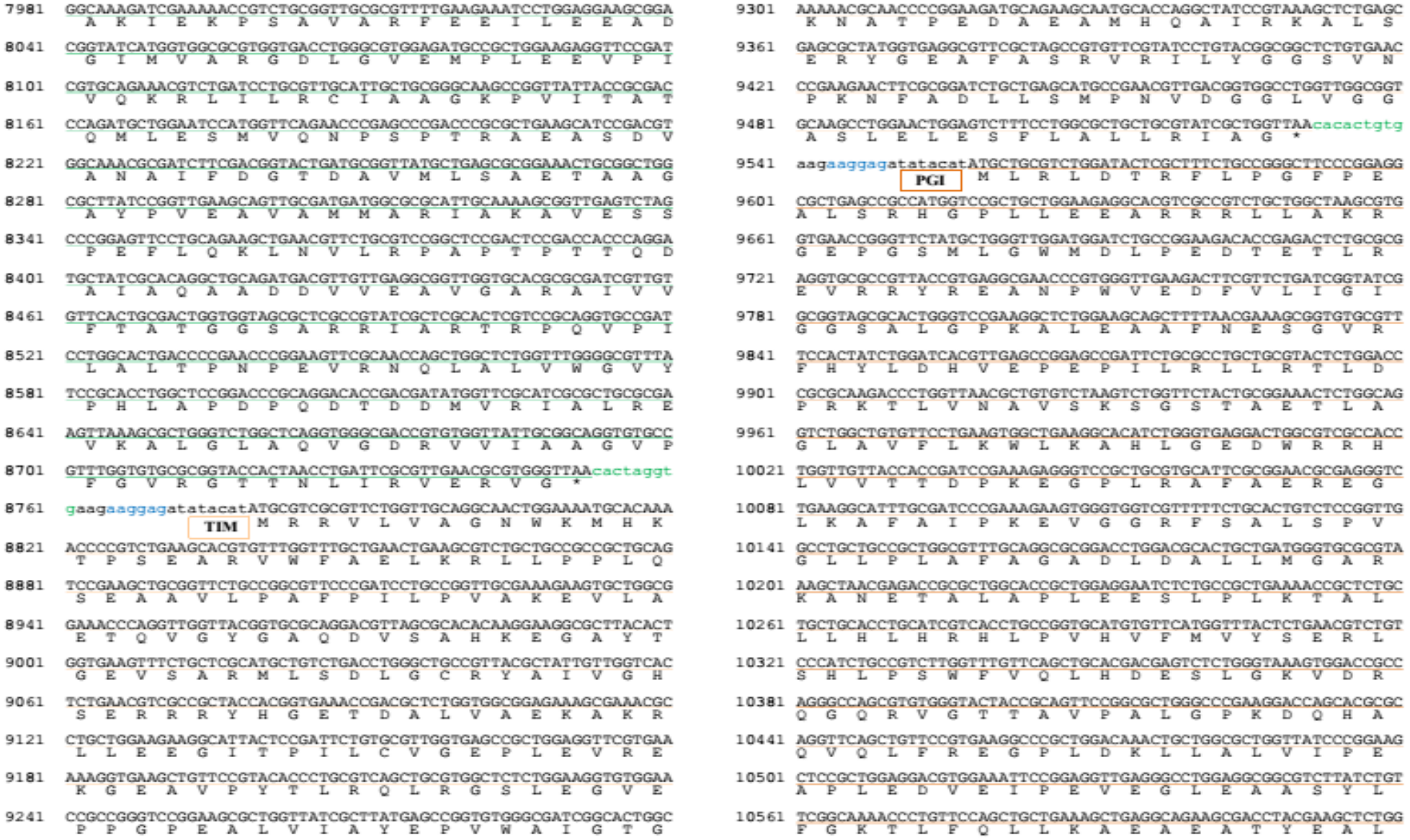
TIM
PGI

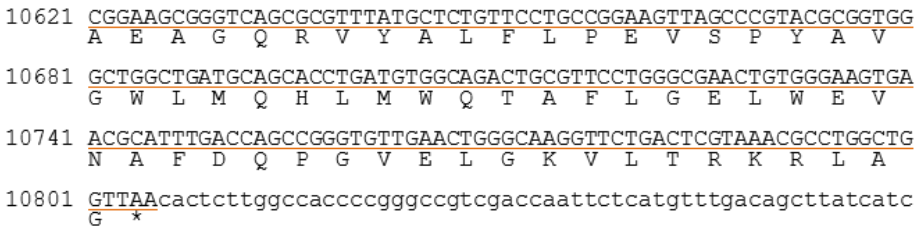

Figure S1. Nucleotide sequence of the artificial operon encoding the nine thermophilic enzymes involved in the chimeric glycolytic pathway. The Pr promoter region was shown in italic letters. *Dra*III restriction sites and the ribosome binding sites were indicated by green and blue letters, respectively. The open reading frames encoding the thermophilic enzymes were underlined.

Supplementary figure S2

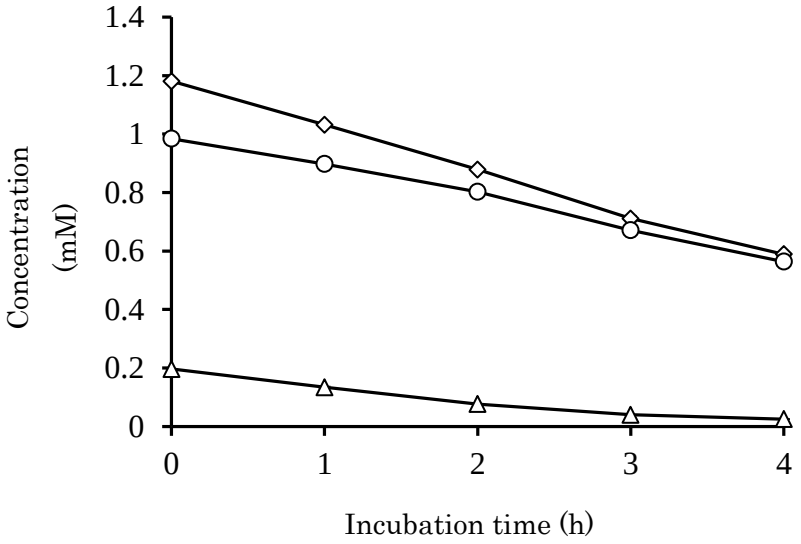

Figure S2. Thermal decomposition of the redox cofactors. A mixture of NAD^+ (1 mM, indicated by circles) and NADH (0.2 mM, triangles) in 50 mM HEPES-NaOH (pH7.0) was incubated at 70°C for indicated time. Residual concentrations of the cofactors were determined by HPLC as described elsewhere (Morimoto et al., 2014). Diamonds indicate the total concentration of NAD^+ and NADH. Data represent the averages of triplicate assays.

Supplementary reference.

Morimoto Y, Honda K, Ye S, Okano K, Ohtake H. 2014. Directed evolution of thermotolerant malic enzyme for improved malate production. J Biosci Bioeng 117:147-152.

Related Publications

1. **Ninh PH**, Honda K, Yokohigashi Y, Okano K, Omasa T, Ohtake H. 2013. Development of a continuous bioconversion system using a thermophilic whole-cell biocatalyst. Appl Environ Microbiol 79:1996-2001.

2. **Ninh PH**, Honda K, Sakai T, Okano K, Ohtake H. 2014. Assembly and multiple gene expression of thermophilic enzymes in *Escherichia coli* for *in vitro* metabolic engineering. Biotechnol Bioeng (in press).

Presentations in Conferences

1. **Ninh PH**, Honda K, Yokohigashi Y, Okano K, Ohtake H. Direct use of recombinant *Escherichia coli* having thermophilic enzyme as whole cell biocatalyst in continuous bioconversion system. JSPS-NRCT young scientist seminar, August 4-5, 2013, Osaka, Japan (Oral presentation).

2. **Ninh PH**, Honda K, Yokohigashi Y, Okano K, Ohtake H. Development of continuous bioconversion system using thermophilic whole-cell biocatalyst. Enzyme Engineering XXII: Emerging topics in enzyme engineering, September 22-26, 2013, Toyama, Japan (Poster presentation).

3. **Ninh PH**, Honda K, Yokohigashi Y, Okano K, Ohtake H. Development of continuous bioconversion system using thermophilic whole-cell biocatalyst. SCEJ 78th Annual Meeting, March, 2013, Osaka, Japan (Oral presentation).

ACKNOWLEDGEMENTS

Completion of this doctoral dissertation was possible with the support of several people. I would like to express my sincere gratitude to all of them. First of all, I am extremely grateful to my supervisor, Prof. Dr. Hisao Ohtake for his fundamental role in my doctoral work. I am deeply grateful for his continuous support and insight. I would like to acknowledge Prof. Dr. Satoshi Harashima and Prof. Dr. Takuya Nihira for their valuable comments and suggestions to improve my thesis. My deepest appreciation comes to my principal supervisor, Assoc. Prof. Kohsuke Honda for every bit of his guidance, assistance, and expertise that I needed during my PhD course.

I am in debt to Dr. Kenji Okano for his advices and assistant in my research. The author is very grateful Dr. K. Tsuge (Institute for Advanced Biosciences, Keio University) for donating plasmid vectors and for technical assistance in gene assembly. I also would like to thank Dr. Y. Muranaka (Research Center for Ultra-High Voltage Electron Microscopy, Osaka University) for his technical assistance in the electron microscopic analysis. I also thanks to Dr. Takashi Mimitsuka (Toray Industries, Inc.) for kindly donating the cell-separation membrane filter.

I sincerely thank all members of Ohtake Laboratory for their helps and encourages. I would like to thank Japanese Government for their financial support during my PhD course.

Finally, to my family: words cannot express how grateful I am for your unconditional love and support. I could not have completed this thesis without you.